10.1071/CH09339
CSIRO 2010 1
Australian Journal of Chemistry, 2010, 63(3), 490-501

An Alternative Platform for the Assessment of Hückel and Möbius Transition States in Concerted Reactions

Kurt H.R. Hennigar[A] *and Richard F. Langler*[B,C]

[A]Arbutus Software, 270-6450 Roberts St., Burnaby British Columbia V5G 4E1

[B]Department of Chemistry, Mount Allison University, Sackville, New Brunswick E4L 1G8

[C]Corresponding author. Email: rlangler@mta.ca

Abstract

A novel approach to the evaluation of Hückel and Möbius transition states is described. It employs incipient π-bond orders, ${}^{o}p_{i,k}$ and ${}^{*}p_{i,k}$. A complete analytical scheme is developed for monocyclic p-orbital arrays in both Hückel and Möbius transition states for both thermal and photochemical reactions. Assessment of monocyclic transition states does not require the calculation of explicit incipient π-bond orders. Transition states featuring polycyclic p-orbital arrays may be assessed by means of calculated ${}^{o}p_{i,k}$ and ${}^{*}p_{i,k}$ values.

Key words: Concerted reactions, Free Electron Model, embedding, π-bond orders.

Introduction

Three major approaches have been developed to predict outcomes for concerted reactions controlled by orbital symmetry – analysis using (i) correlation diagrams,[1] (ii) frontier-orbital interactions in transition states,[2] and (iii) aromatic/antiaromatic character for p-orbital arrays in transition states (Hückel/Möbius).[3-5] Electrocyclic reactions, cycloaddition reactions, sigmatropic rearrangements, cheletropic expulsions and carbene insertions are included in the set of reaction types the aforementioned analyses have helped chemists to understand. Discussion, herein, will focus on electrocyclic reactions, although the analytical protocol we advance can be readily applied to any of the reaction types just listed.

The simplicity of the Hückel/Möbius approach makes it particularly attractive for routine use. Consider the electrocyclic reaction which interconverts hexatriene **1** and cyclohexadiene **2** (see Scheme 1).

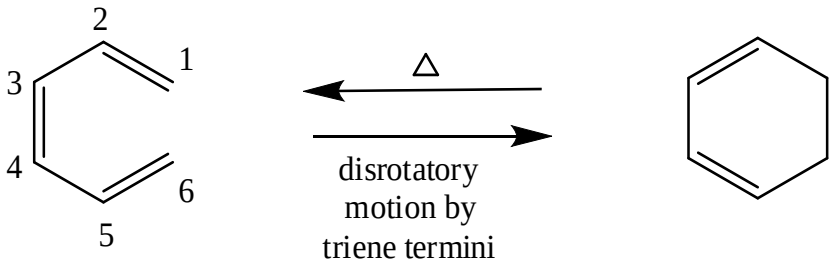

1 **2**

Scheme 1. An exemplary electrocyclic reaction.

A drawing of the p-orbital array in the transition state, accompanied by a routine Hückel/Möbius evaluation is presented in Figure 1.

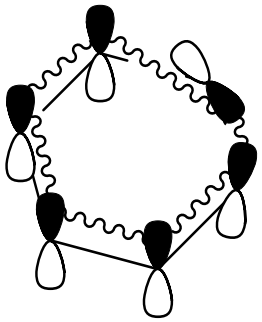

0 nodes, Hückel array
4J+2 π electrons, aromatic
Δ allowed
hν forbidden

Fig. 1. Routine analysis of the transition state for disrotatory closure of hexatriene **1** leading to the conclusion that this pathway (Scheme 1) is a thermally allowed but photochemically forbidden one. The wavy lines indicate orbital overlap.

The exemplary Hückel/Möbius assessment, portrayed in Figure 1, rests upon the analogy between the hexatriene **1** transition state for disrotatory closure (Fig. 1) and benzene's ground state. The critical feature of the reference annulene's ground state is whether it is open-shell or closed-shell at the Hückel level.[6] Hückel annulenes can have their Hückel-level ground-state multiplicities conveniently determined by means of the Frost-Musulin circle mnemonic.[7] Möbius annulenes can have their Hückel-level ground-state multiplicities conveniently determined by means of the Zimmerman circle mnemonic.[8]

Problems

Neither the Frost-Musulin nor the Zimmerman mnemonics can be applied to substituted annulenes, so that each Hückel/Möbius transition state analysis implicitly requires one to identify

a monocyclic p-orbital array as a prerequisite for assessment. Orbitals outside the monocyclic array must be ignored when they are situated on simple even or *odd* acyclic chains. Moreover, complex polycyclic π-systems must be largely ignored in these transition state assessments. Some commonplace problems lead to capricious choices between which p-orbital array to focus on and which to ignore.

A familiar example is the electrocyclic transformation of cyclooctatetraene **3** into the bicyclooctatriene **4** shown in Scheme 2.

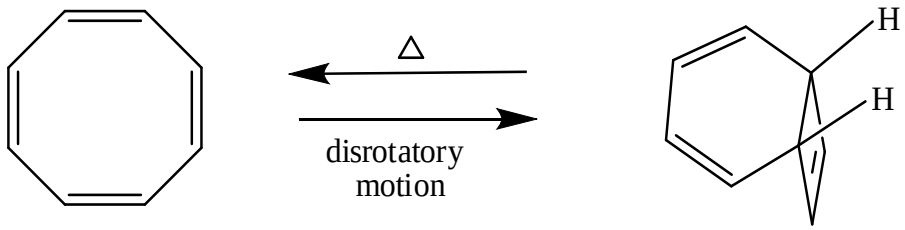

3 **4**

Scheme 2.

Disrotatory closure/opening to interconvert **3** and **4** provides a p-orbital array, like that in Figure 1, for the newly-forming 6-membered ring and so is thermally allowed. However, disrotatory closure also provides the monocyclic p-orbital array pictured in Figure 2 for the newly-forming 4-membered ring which leads to the conclusion that disrotatory closure is thermally forbidden.

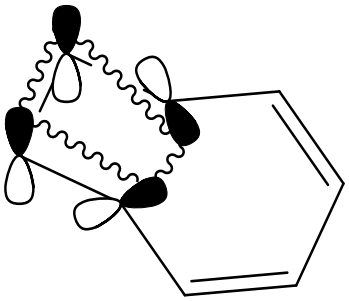

0 nodes, Hückel array
4J π electrons, antiaromatic
Δ forbidden
hν allowed

Fig. 2. Routine Hückel/Möbius analysis of the transition state for the disrotatory closure pictured in Scheme 2. The wavy lines indicate orbital overlap.

Clearly the foregoing analyses of thermal disrotatory closure for **3** are unsatisfactory. An examination of conrotatory closure for **3** fares no better with the established Hückel/Möbius approach.

Of the three approaches to concerted symmetry-controlled reactions, only the Hückel/Möbius approach offers no explicit assessment of transition states for photolyses. This deficiency is disappointing and intrinsically sets aside the possibility that there may be concerted reactions which proceed, both thermally and photochemically, to give the same stereochemistry.

The application of a correlation diagram to the assessment of a concerted reaction is formally limited to one for which symmetry is conserved throughout the reaction. Hence, there are many reactions for which correlation diagrams can not be constructed.

Following from the Klopman-Salem equation,[9-11] frontier-orbital arguments[2] focus on the pre-eminent role of those orbitals and their electrons in determining the outcome of concerted reactions, often, to the exclusion of all other orbital/electron interactions. Since non-frontier

orbitals and their electrons can have observable consequences for the outcome of chemical reactions, it might be advantageous to have access to an approach to transition-state assessments that allows for the effect of non-frontier electrons/orbitals on transition-state viability.

The following material attempts to address all of these problems.

Methods

Simple Hückel calculations were carried out in the usual way assuming the orthogonality of adjacent p-orbitals (i.e. assuming they fail to overlap). PM3 calculations were carried out as described earlier.[12]

The Free Electron Model (FEM) provides the Hückel-level molecular orbital coefficient $a_{m,b}$ for any vertex C_m in any π-molecular orbital, Ψ_b, for any odd or even unbranched acyclic hydrocarbon π-system.[13,14] For even, unbranched, acyclic hydrocarbons (2n polyenes), coefficients may be obtained from Eqn (1).

$$a_{m,b} = \sin[bm180^{\circ}(2n+1)^{-1}] \quad (1)$$

No FEM coefficient for a given, unbranched, acyclic 2n polyene is normalized. But, when an FEM coefficient is multiplied by the normalization coefficient, y_e [see Eqn (2)], it will be transformed into the more familiar Zeroth Order Hückel coefficient.

$$y_e = (n+0.5)^{-0.5} \quad (2)$$

For odd, acyclic, unbranched hydrocarbons (2n+1 polyenyls), FEM coefficients may be obtained from Eqn (3).

$$a_{m,b} = \sin[bm180^{\circ}(2n+2)^{-1}] \quad (3)$$

To transform the FEM coefficient for a 2n+1 polyenyl vertex into the more familiar normalized

Hückel coefficient, $a_{m,b}$ should be multiplied by the appropriate normalization coefficient, y_o [see Eqn (4)].

$$y_o = (n+1)^{-0.5} \quad (4)$$

Glossary

1. J, N, j, i, n and f may be any natural number.

2. $a_{m,b}$ is the molecular orbital coefficient for C_m in Ψ_b.

3. R_q represents the number of carbon atoms (q) in a newly-forming (incipient) or fully-formed ring.

4. At the Hückel level, each atom in a given π-system has a set of coefficients, one for each molecular orbital. A string is a subset of those coefficients, insulated from the next string by a zero coefficient.

5. A Hückel array of p-orbitals must form a closed loop and may have any even number of nodes.[8]

6. A Möbius array of p-orbitals must form a closed loop and may have any odd number of nodes.[8]

7. ${}^{o}p_{i,k}$ is the π-bond order between non-adjacent vertices C_i and C_k in any hydrocarbon π-system. ${}^{*}p_{i,k}$ is the corresponding quantity for the lowest-lying photoexcited state.

8. A pair of isoconjugate neutral hydrocarbons have identical numbers of p-orbitals in their respective π-systems.

9. A *simple* linear combination of small polyene/polyenyl molecular orbitals has (i) each nearest-neighboring pair of small orbital segments insulated from each other by a zero coefficient and (ii) coefficient ratios within each segment that match those in the molecular orbital of the small polyene.

10. For a neutral polyene which has no non-bonding molecular orbitals, the E_π value is obtained by summing the eigenvalues for the bonding orbitals and then doubling the total.

Results and Discussion

In addition to the problems presented by the current Hückel/Möbius approach outlined in the Introduction, it is easy to entertain serious reservations about the description of a small Möbius annulene as aromatic. Heilbronner,[15] the first to examine Möbius annulenes at the Hückel level, acknowledged that only relatively large rings (e.g. R_{20}) could achieve the twisted structures he envisioned. In contrast to the Hückel-level results for it, a PM3 computational examination of Möbius cyclobutadiene[6] found that it (i) is chiral, (ii) has no C_2 axis, (iii) has no degenerate molecular orbitals (iv) is not a ground-state singlet, (v) has a significant dipole moment and (vi) is not even a local energy minimum. Möbius cyclobutadiene is not aromatic. If small Möbius annulenes are unsuitable reference structures for the assessment of transition states, it might be fruitful to look elsewhere for a method to assess transition states. We have elected to explore starting-material properties that might reasonably be extended to transition states. Unbranched polyene/polenyl π-bond orders were selected as measures of systematic preferences for competing electrocyclic closures. We refer to π-bond orders between non-adjacent vertices in a given polyene as ${}^{o}p_{i,k}$ values. The superscript is meant to indicate that the π-bond order applies to the hypothetical process in which a new C_i-C_k bond begins to form and an incipient ring begins to take shape. A noteworthy feature of ${}^{o}p_{i,k}$ values for transition state assessment is that they avoid direct dependence on Hückel-level energies which are known to be unreliable.

Application of the FEM to Incipient Rings in Hückel Transition States

${}^{o}p_{i,k}$ Values for Incipient α,ω Closure of Neutral Unbranched Polyenes

Figure 3 presents a generalized form of the π-molecular orbitals for hexatriene **1** which can be readily anticipated by application of the FEM [see Eqn (1) in Methods].

C_6	a	-b	c	-c	b	-a
C_5	b	-c	a	a	-c	b
C_4	c	-a	-b	b	a	-c
C_3	c	a	-b	-b	a	c
C_2	b	c	a	-a	-c	-b
C_1	a	b	c	c	b	a
	Ψ_1	Ψ_2	Ψ_3	Ψ_4	Ψ_5	Ψ_6

Fig. 3. Generalized FEM coefficients for the π-molecular orbitals of hexatriene **1**.

From Eqn (1), it follows that the molecular orbital coefficient $a_{m,b}$ equals the molecular orbital coefficient $a_{b,m}$. This leads to a useful mapping operation for acyclic unbranched polyene coefficients displayed in the manner shown in Figure 3. *Each set of molecular orbital coefficients (e.g. each column in Fig. 3) is symmetric with respect to clockwise rotation, by 90˚, about the $a_{x,x}$ coefficient in the set.* As an example, when column 2 (Ψ_2 coefficients) is so rotated about the $a_{2,2}$ coefficient (c), it is mapped onto the set of C_2 coefficients with which it is congruent. Hence, generally the π-molecular orbital coefficients for Ψ_x which are allocated one to each carbon atom in the π-system, are identical to the π-molecular orbital coefficients for C_x which are allocated one to each molecular orbital associated with the unbranched acyclic polyene of interest. From Eqn (1), Ψ_1 coefficients will increase in magnitude a → b →c… and the absolute value of the frontier orbital coefficients (e.g. c in Fig. 3) will be less than 1.

Rotation of column 1 about $a_{1,1}$ leads to the conclusion that C_1 will always have Ψ_1 coefficients distributed over all of the polyene molecular orbitals. Either from Eqn (1) or from a symmetry argument, C_{2n} in any unbranched, acyclic polyene will have coefficients with the same

absolute value as those for C_1 but the C_{2n} coefficients will alternate their signs. In general, ${}^{o}p_{i,k}$ values for such systems will be composed of a series of coefficient squares which will have alternating signs and whose absolute values will increase steadily. The generalized ${}^{o}p_{i,k}$ expression for α,ω incipient ring formation for hexatriene **1** (see Fig. 1) is given in Eqn (5).

$$ {}^{o}p_{1,6} = 2(a^2\text{-}b^2 + c^2) > 0 \qquad (5) $$

Incipient α,ω closure for a C_{2n} polyene (if n is odd) leads to an unsubstituted 4J+2 ring, ${}^{o}p_{\alpha,\omega} > 0$ and a favorable transition state. In contrast, incipient α,ω closure for a C_{2n} polyene (if n is even) leads to an unsubstituted 4J ring, ${}^{o}p_{\alpha,\omega} < 0$ and an unfavorable transition state. The generalized ${}^{o}p_{i,k}$ expression for α,ω incipient ring formation for octatetraene **5** (Fig. 4) is given in Eqn (6).

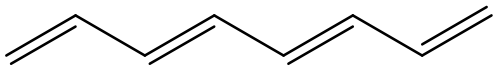

5

Fig. 4.

$$ {}^{o}p_{1,8} = 2(a^2\text{-}b^2 + c^2 - d^2) < 0 \qquad (6) $$

Based on ${}^{o}p_{\alpha,\omega}$ values, thermal reactions proceeding through Hückel arrays with 4J+2 π electrons will always be favored whereas the corresponding 4J transition states will always be disfavored when the cyclic transition state is *unsubstituted*.

$^{o}p_{i,k}$ Values for Incipient α,ω Closure of Charged Polyenes

If an unbranched acyclic polyene gains a pair of electrons, they must go into the LUMO (Lowest Unoccupied Molecular Orbital). In calculating the $^{o}p_{i,k}$ values for the newly-formed dianion, the LUMO will contribute a term that is equal in magnitude but opposite in sign to that contributed by the HOMO (Highest Occupied Molecular Orbital). As an example, Eqn (7) gives the $^{o}p_{1,8}$ expression for incipient α,ω closure of the octatetraene dianion, $\mathbf{5}^{2-}$.

$$^{o}p_{1,8}]^{2-} = 2(a^2 - b^2 + c^2 - d^2 + d^2) = 2(a^2 - b^2 + c^2) > 0 \qquad (7)$$

While α,ω closure for octatetraene **5** has a disfavored transition state [(see Eqn (6)], α,ω closure for the octatetraene dianion, $\mathbf{5}^{2-}$ has a favored transition state [see Eqn (7)]. Whenever the HOMO of the neutral, unbranched polyene diminishes $^{o}p_{\alpha,\omega}$, closure of the dianion through a Hückel p-orbital array will be facilitated. Whenever the HOMO of the neutral, unbranched, acyclic polyene increases $^{o}p_{\alpha,\omega}$, closure of the dianion through a Hückel transition state will be impaired.

One can decide what to expect, for a given polyene, by considering the nodal properties of the appropriate HOMO. "The HOMO nodal pattern may be rapidly generated by bringing together a set of ethylene HOMOs so that each contact point introduces a phase dislocation."[16] Figure 5 presents inicipient α,ω closure for decapentaene **6** and the corresponding dianion $\mathbf{6}^{2-}$.

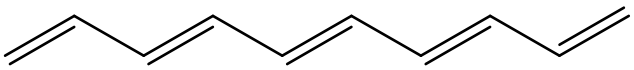

6

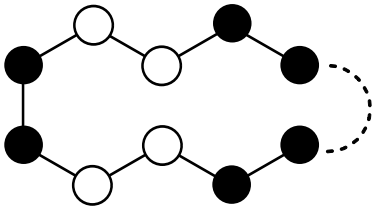

HOMO contribution to ${}^{o}p_{1,10} > 0$
neutral polyene closure facitiltated
corresponding dianion closure impaired

Fig. 5. Relative facilities of transition-state formation for α,ω closure of decapentaene **6** and its dianion $\mathbf{6}^{2-}$.

If an unbranched, acyclic polyene loses a pair of electrons, they must come from the HOMO. Thus, again, the impact of the HOMO contribution to ${}^{o}p_{i,k}$ is eliminated in the doubly charged species. The dication expression ${}^{o}p_{1,8}]^{2+}$ for the octatetraene dication $\mathbf{5}^{2+}$ is identical to the right-hand side of Eqn (7). One could then add to Figure 5 – "corresponding dication closure impaired".

General conclusions can now be reached for thermal transition state formation for α,ω cyclization of polyenes with 4J or 4J+2 π electrons and their corresponding doubly-charged ions through Hückel p-orbital arrays: $4J^{2+}$ or $4J^{2-}$, favored; 4J, disfavored; $4J+2^{2+}$ or $4J+2^{2-}$, disfavored; 4J+2, favored.

${}^{o}p_{i,k}$ Values for Incipient α,ω Closure of Neutral, Unbranched Polyenyls

Figure 6 presents a generalized form for the π-molecular orbitals for pentadienyl **7** which can be readily anticipated by application of the FEM [see Eqn (3)].

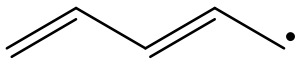

7

C_5	a	-b	1	-b	a
C_4	b	-b	0	b	-b
C_3	1	0	-1	0	1
C_2	b	b	0	-b	-b
C_1	a	b	1	b	a
	Ψ_1	Ψ_2	Ψ_3	Ψ_4	Ψ_5

Fig. 6. Generalized FEM coefficients for the π-molecular orbitals of pentadienyl **7**. FEM coefficients are not normalized (see Methods).

Unbranched, acyclic polyenyl coefficients, displayed in the manner employed in Figure 6, have rotational symmetry as discussed for acyclic, unbranched polyene coefficients (see Fig. 3 and attendant discussion). Unlike polyenes, C_{2n+1} polyenyls each have a central carbon, C_{n+1}. From Eqn (3), when bm = f(n+1), where f is any odd natural number, $a_{n+1} = \pm 1$ but when f is any even natural number, $a_{n+1} = 0$. In applying the FEM for unbranched, acyclic polyenyl coefficient tables (e.g. Fig. 6), one can begin by filling in the coefficients for C_{n+1} and Ψ_{n+1}.

Consider α,ω closure for C_{2n+1} polyenyls. π-Bond order expressions would have the same form as those for the α,ω closure of polyenes plus a term, ±1, to account for the SOMO (Singly Occupied Molecular Orbital) contribution. Note that the factor 2 accounts for the double occupancy of the π orbitals in Eqns (5) → (7). Since the SOMO of the C_{2n+1} is only singly occupied, the product of the α and ω coefficients is only multiplied by 1 to determine its contribution to ${}^{o}p_{\alpha,\omega}$. Eqn (8) presents a generalized form of the ${}^{o}p_{1,7}$ calculation for heptatrienyl **8** (Fig. 7).

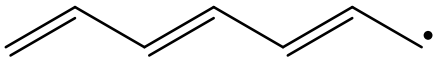

8

Fig. 7.

$$^{o}p_{1,7} = 2(a^2-b^2+c^2) - 1 \qquad (8)$$

Since, for a given hydrocarbon, the sum of the squares of the coefficients for one orbital must equal the sum of the squares of any other orbital, one can say that the sum of the Ψ_1 coefficient squares equals the sum of the Ψ_2 coefficient squares for heptatrienyl **8** [see Eqn (9)].

$$2a^2 + 2b^2 + 2c^2 + 1 = 4b^2 + 2 \qquad (9)$$

From Eqn (9), it follows that Eqn (8) equals zero. In this simple way, one can show that all acyclic, neutral, unbranched polyenyls have $^{o}p_{\alpha,\omega}$ values of zero.

$^{o}p_{i,k}$ Values for Incipient α,ω Closure of Charged, Unbranched Polyenyls

For C_{2n+1} polyenyls, if n is an odd natural number (4J+3 π electrons), the SOMO contribution to $^{o}p_{\alpha,\omega}$ is always -1. If the neutral polyenyl gives up an electron, $^{o}p_{\alpha,\omega}$ is increased to +1 and the thermal transition state (Hückel array) is favored. If the polyenyl gains an electron, $^{o}p_{\alpha,\omega}$ is decreased to -1 and the thermal transition state (Hückel array) is disfavored. Similarly, for 2n+1 polyenyls, if n is an even natural number (4J+5 π electrons), the SOMO contribution to $^{o}p_{\alpha,\omega}$ is always +1. From here charge effects are readily anticipated.

The form of the SOMO (non-bonding molecular orbital) is easily deduced from the Pairing Theorem for odd alternant hydrocarbons.[17] As was the case for the polyenes, the frontier-orbital nodal properties permit facile anticipation of the impact of charge on $^{o}p_{\alpha,\omega}$ values and therefore on incipient ring formation. Figure 8 presents nonatetraenyl **9** as a case in point.

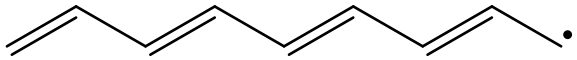

9

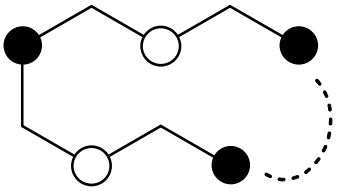

SOMO contribution to ${}^{o}p_{1,9} > 0$
anionic polyenyl closure favored
cationic closure disfavored

Fig. 8. Relative facilities of transition-state formation for α,ω closure of the nonatetraenyl **9**-derived cation and anion.

General conclusions can now be reached for thermal Hückel transition-state formation for α,ω closure of polyenyl ions derived from the 4J+3 and 4J+5 polyenyls: $4J+5^{-}$ or $4J+3^{+}$, favored; $4J+5^{+}$ or $4J+3^{-}$, disfavored.

${}^{o}p_{i,k}$ *Values for Selected Non-α,ω Incipient Closures of Neutral, Unbranched Polyenes (Hückel Transition States)*

The following sections establish a straightforward way to evaluate competing monocyclic transition states for incipient, alternant rings that bear unbranched, acyclic substituents, either odd or even.

Embedding Acyclic, Unbranched Polyenes

Some polyenyls have Hückel-level π-molecular orbitals that are simple linear combinations of the π-molecular orbitals associated with smaller polyenes or polyenyls. Figure 6 shows that Ψ_2 and Ψ_4 are simple linear combinations of ethylene molecular orbitals. Similarly, some polyenes have orbitals of this type. Figure 9 shows the nodal properties of a pair of octatetraene **5**

π-molecular orbitals that are linear combinations of ethylene π-molecular orbitals.

Fig. 9. A pair of octatetraene **5** Hückel molecular orbitals that are simple linear combinations of ethylene π-molecular orbitals.

Both pentadienyl **7** and octatetraene **5** have skeletal segments, each of which houses the molecular orbital from a smaller structure and insulating vertices, each of which has a zero coefficient in that molecular orbital. The process of recognizing such orbital relationships is called embedding.[18]

Embedding demands, in addition to recognizing that a given hydrocarbon framework can accommodate the smaller π molecular orbitals and insulating vertices (zero coefficients), that those non-zero coefficients attached to a common zero must add up to zero (Zero Sum Rule). Unlike more complex structures, whenever an acyclic, unbranched polyene framework can accomodate the smaller molecular orbitals and insulating coefficients, the Zero Sum Rule can always be satisfied.

The novel procedure, developed below, permits rapid identification of embeddable, acyclic, unbranched polyenes, appropriate small π systems to embed for and carbon atoms which have coefficient strings that correspond to the small-structure molecular-orbital coefficients.

For an acyclic, unbranched polyene, the smallest values of b and m associated with a zero coefficient must make the sine function in Eqn (1) equal zero. Since none of the variables b, m and 2n+1 can be zero, if the sine function is to equal zero, Eqn 10 must hold.

$$bm = 2n + 1 \qquad (10)$$

To find the atom/orbital combinations associated with zero coefficients (the hallmark of embeddable polyenes) one has to factor 2n+1 into pairs of odd numbers. As an example, the C_{14} polyene **10** (Fig. 10) has a 2n+1 value of 15 which can be uniquely factored into 5 and 3.

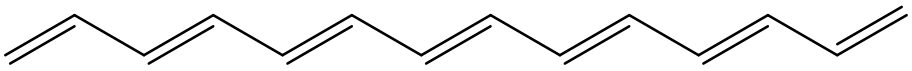

10

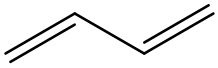

11

Fig. 10.

Hence, both C_3 in Ψ_5 and C_5 in Ψ_3 have zero coefficients. So, Ψ_5 has insulating zero coefficients between C_2 segments and Ψ_3 has insulating zero coefficients between C_4 segments. The C_{14} polyene **10** can be embedded for ethylene and butadiene **11** (Fig. 10). Whenever $bm(2n+1)^{-1}$ provides a natural number, $a_{m,b}$ is zero. Therefore, for the C_{14} polyene **10**, Ψ_3, Ψ_6, Ψ_9 and Ψ_{12} are all linear combinations of the molecular orbitals associated with butadiene **11**. Moreover, C_3, C_6, C_9 and C_{12} have FEM coefficient strings that correspond to linear combinations of butadiene Ψ_1, Ψ_2, Ψ_3 and Ψ_4 FEM coefficients respectively. Similarly, C_5 and C_{10} have coefficient strings that correspond to linear combinations of ethylene Ψ_1 and Ψ_2 FEM coefficients respectively. Whenever 2n+1 is a prime number the appropriate unbranched, acyclic polyene cannot be embedded e.g. decapentaene **6** has a 2n+1 value of 11 and cannot be embedded.

$^{o}p_{i,k}$ Values for Non-α,ω Polyene Closures: Disubstituted Incipient Rings

In order to obtain unambiguous generalized $^{o}p_{i,k}$ values for infinite sets of substituted, incipient polyenes, it is essential to have simple expressions whose relative values are immediately obvious upon inspection. Embeddable polyenes are particularly attractive for this purpose because those orbitals which are simple linear combinations of smaller molecular orbitals lead to carbon atoms whose coefficient sets feature zeros, thereby providing simpler expressions for all of their π-bond orders. Furthermore, those atoms are associated with coefficient strings whose absolute values repeat from string to string which can lead to substantial additional simplification for some of their π-bond orders. Shorter strings minimize the number of unknowns and maximize the number of zeros in the subset of coefficients an appropriate atom has in its bonding molecular orbitals. String lengths of four, found for atoms that correlate with molecular orbitals which are linear combinations of butadiene **11** molecular orbitals, are sufficiently short to produce unambiguous $^{o}p_{i,k}$ expressions and sufficiently long to permit access to assessments for all disubstituted, monocyclic, alternant transition states.

Unbranched, acyclic polyenes featuring 10N+14 carbon atoms constitute an endless set of polyenes, each of which can be embedded for butadiene **11**. The lowest-lying 10N+14 polyene molecular orbital that is a simple linear combination of butadiene orbitals (Ψ_1) is Ψ_{2N+3}. Thus, C_{2N+3}, C_{4N+6}, C_{6N+9} and C_{8N+12} have coefficient strings that correspond to butadiene **11** Ψ_1, Ψ_2, Ψ_3 and Ψ_4 FEM coefficients, respectively. Using these carbon atoms, disubstituted incipient ring sizes for which unambiguous $^{o}p_{i,k}$ values are available from any 10N+14 acyclic, unbranched polyene are: unsymmetrical R_{2N+4}, R_{4N+7}, R_{6N+10} and symmetrical R_{2N+4}. The unsymmetrical 2N+4 incipient rings will bear a pair of adjacent, even substituents and the symmetrical one will bear a pair of adjacent odd substituents.

If, as is often the case, a 10N+14 polyene can be embedded for other small π systems, there will be additional incipient rings whose generalized ${}^{o}p_{i,k}$ expressions can be unambiguously assessed. As an example, the C_{44} unbranched, acyclic polyene can be embedded for C_2, C_4, C_8 and C_{14} π systems which leads to 57 unambiguous ${}^{o}p_{i,k}$ expressions only six of which come from carbon strings of length four.

Figure 11 depicts incipient rings and their ${}^{o}p_{i,k}$ values (calculated from C_{2N+3}, C_{4N+6}, C_{6N+9} and C_{8N+12}) for the 10N+14 polyene cases where N = 0 or N = 1.

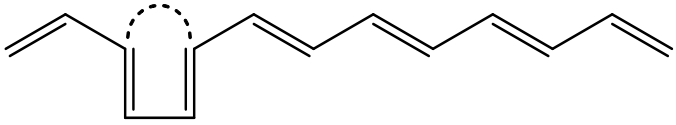

R_4; ${}^{o}p_{i,k} = -4cf << 0$

10a

R_4; ${}^{o}p_{i,k} = 2c^2 - 2f^2 < 0$

10b

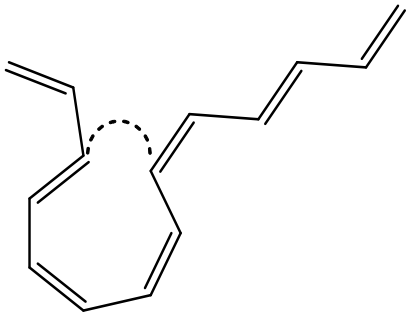

R_7; ${}^{o}p_{i,k} = 0$

10c

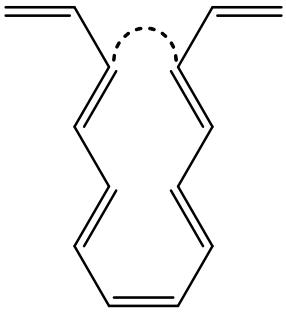

R_{10}; ${}^{o}p_{i,k} = -2c^2 + 2f^2 > 0$

10d

Fig. 11. Part 1.

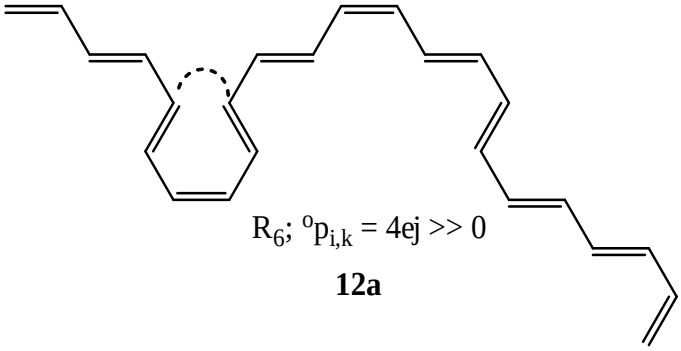

R_6; ${}^{o}p_{i,k} = 4ej >> 0$

12a

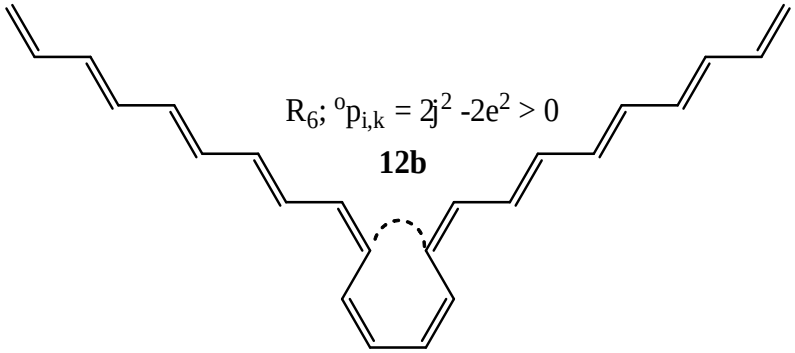

R_6; ${}^{o}p_{i,k} = 2j^2 - 2e^2 > 0$

12b

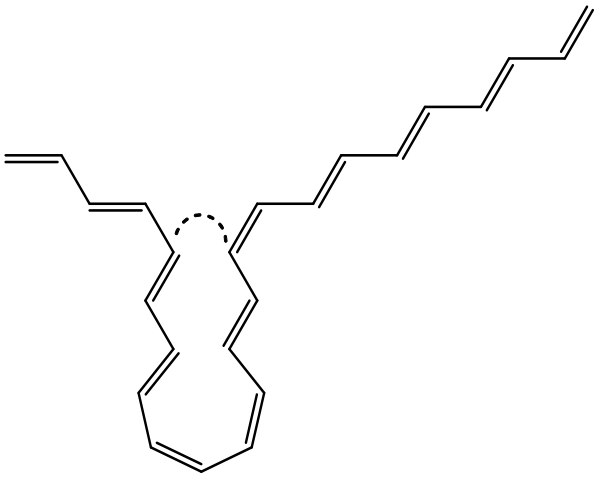

R_{11}; ${}^{o}p_{i,k} = 0$

12c

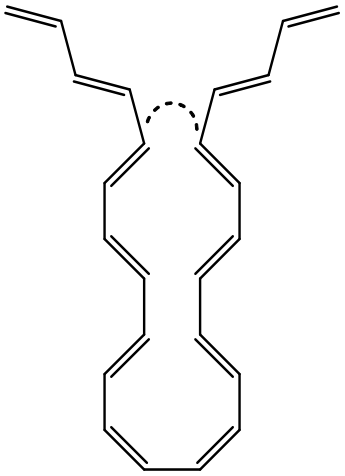

R_{16}; ${}^{o}p_{i,k} = -2j^2 + 2e^2 < 0$

12d

Fig. 11. Incipient ring formation for two sets of 10N+14 polyenes, N = 0 (**10a - 10d**) and N = 1 (**12a - 12d**).

Note that each non-alternant transition state in Figure 11 has a ${}^{o}p_{i,k}$ value of zero in accord with what was established for their ${}^{o}p_{\alpha,\omega}$ values for neutral, unbranched polyenyls.

Because the absolute value of the coefficients increases as the letters in the ${}^{o}p_{i,k}$ expressions ascend the alphabet, comparison of the relative magnitudes of those expressions for a given value of N are straightforward for some isoconjugate pairs e.g. **10b** and **10d** (Fig. 11). The relative magnitudes of ${}^{o}p_{i,k}$ values, obtained directly from FEM coefficients, which have the forms $\pm 4xz$ and $\pm(2x^2 - 2z^2)$ may not be immediately obvious. From the form of butadiene **11** Ψ_1 and Ψ_2 orbitals, the C_1 coefficient in Ψ_{2N+3} is x and the C_1 coefficient in Ψ_{4N+6} is z. For all 10N+14 polyenes, x is sin(36˚) and z is sin(72˚). Ergo, for any given N value, these ${}^{o}p_{i,k}$ values will have the relative magnitudes given in Eqn (11).

$$|4xz| > |2x^2 - 2z^2| \qquad (11)$$

Henceforth, ranking these FEM-based ${}^{o}p_{i,k}$ values will present no ambiguity for any value of N. Note that FEM coefficients are not normalized. To obtain normalized coefficients, each FEM coefficient must be multiplied by y_e (see Methods) which is always less than one and shrinks as 2n increases.

From Figure 11, one can assess the impact of substituent parity on transition states for alternant ring formation. Formation of a 4J circuit, for a ring bearing only even substituents, is strongly disfavored (Hückel orbital array). While 4J circuit formation, for a ring bearing a pair of odd substituents, is weakly disfavored when a thermolysis proceeds through a Hückel transition state (see **10a** and **10b** in Fig. 11). A corresponding difference is found for the favored 4J+2 ring formations (**12a** and **12b** in Fig. 11). A pair of odd substituents attenuates but does not qualitatively alter the conclusion regarding the favorability of formation for a given alternant ring type.

Relative to the unsubstituted (α,ω closure) annulene cyclization, appending a pair of odd substituents sharply alters the relative magnitude of the calculated ${}^{o}p_{i,k}$ value. In contrast, appending a pair of even substituents has little obvious effect on the relative magnitude of calculated ${}^{o}p_{i,k}$ values. The present approach offers direct mathematical support for the widespread practice of assuming that even, acyclic substituents may be safely ignored in making predictions about ring formation through concerted reactions. It is now clear that no such assumption is reasonable for the formation of alternant rings bearing a pair of odd, acyclic substituents.

${}^{o}p_{i,k}$ Values for Non-α,ω Polyenyl Closures: Disubstituted Incipient Rings

Like their polyene counterparts, embeddable polyenyls may give unambiguous expressions for ${}^{o}p_{i,k}$ values and, thereby, give convenient assessments for transition-state favorabilities. An unbranched, acyclic polenyl has a molecular orbital (Ψ_b) with a zero coefficient at C_m when Eqn (12) holds.

$$bm = f(2n+2) \qquad (12)$$

Again, successful embedding for butadiene **11** gives the best combination of simple ${}^{o}p_{i,k}$ expressions and alternant ring types in subject transition states. Acyclic, unbranched polyenyls with 10N+9 skeletal carbon atoms can be so embedded. Polyenyl molecular orbitals Ψ_{2N+2}, Ψ_{4N+4}, Ψ_{6N+6}, Ψ_{8N+8} are linear combinations of butadiene **11** Ψ_1, Ψ_2, Ψ_3 and Ψ_4 π-molecular orbitals, respectively. Hence, C_{2N+2}, C_{4N+4}, C_{6N+6} and C_{8N+8} have coefficient strings whose values match those of the butadiene **11** FEM molecular orbital coefficients found in the appropriate orbitals.

As for the polyenes, complete C_4 strings (strings that are associated with bonding molecular orbitals), for any pair of vertices listed above, contribute nothing to ${}^{o}p_{i,k}$. Non-α,ω non-alternant

incipient rings initiate a bonding interaction to which the SOMO contributes nothing. Hence, for polyenyls, if a non-alternant transition state forms a disubstituted ring which bears a pair of odd substituents, neither the corresponding cation nor the corresponding anion closure is facilitated. This conclusion can be easily reached from the polyenyl SOMO. As an example, any closure of nonateraenyl **9** to form a non-alternant ring leads to no SOMO-derived stabilization regardless of the number of SOMO electrons (see Fig. 8 and examine incipient bonding between any even pair of carbon atoms).

Figure 9 provides a comparison of unsubstituted and disubstituted anionic R_5 transition states.

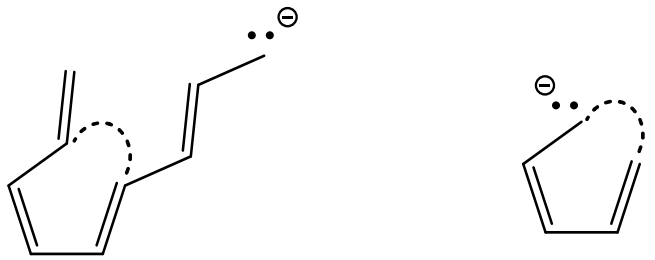

remains unfavored in spite of charge	favored because of charge

Fig. 12.

Unbranched, acyclic neutral polyenyl frameworks provide results for alternant ring formation that are comparable to those already discussed for polyene incipent ring formation. Consider $^{o}p_{1,n+1}$ values for 8N+7 unbranched, acyclic polyenyls. All incipient closures produce 4J rings and all $^{o}p_{1,n+1}$ values are less than zero (thermally disfavored through Hückel arrays). Eqn (13) gives the $^{o}p_{1,4}$ value for the N = 0 system.

$$^{o}p_{1,4} = 2a - 2c < 0 \qquad (13)$$

Consider 8N+11 unbranched, acyclic polyenyls. All incipient 1,n+1 closures produce 4J+2 rings and all $^{o}p_{i,k}$ values are greater than zero (thermally favored through Hückel arrays). Eqn (14) gives the $^{o}p_{1,6}$ value for the N = 0 system.

$$^{o}p_{1,6} = 2a - 2c + 2e > 0 \qquad (14)$$

Up to this point, all of the transition states, both favored and disfavored, have been appropriate for thermal electrocyclic reactions that proceed through disrotatory motion. It is well known that stereochemical evidence implicates conrotatory thermal closures for some substrates. These reactions are discussed in terms of Möbius p-orbital arrays in their transition states.

$^{o}p_{i,k}$ Values and Möbius Transition States

Figure 1 presents a thermally allowed transition state for an electrocyclic closure in which the incipient ring has 4J+2 π electrons. That transition state ensues from disrotatory motion to produce a Hückel p-orbital array (even number of nodes). When conrotatory motion of the termini is pursued, each possible representation of the orbital array in the transition state must have an odd number of nodes. Figure 13 presents such a transition state for butadiene **11** along with a standard Hückel/Möbius assessment.

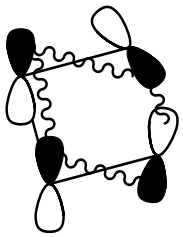

1 node, Möbius array
4J π electrons, aromatic
Δ allowed
hν forbidden

Fig. 13. Routine analysis of the transition state for conrotatory closure of butadiene **11** leading to the conclusion that this pathway is a thermally allowed but photochemically forbidden one. The wavy lines indicate orbital overlap.

In terms of the newly-forming transition-state bond, conrotatory motion, starting from the standard orbital orientation of the p-orbital basis set, leads to increasing antibonding as rotation proceeds. When one of the polyene terminal p-orbitals is inverted, the orbital interaction in the newly-forming bond becomes bonding. Inversion of a p-orbital is indicated by a sign change for its molecular-orbital coefficients. Hence, in sharp contrast to Hückel transition states, a $^{o}p_{i,k}$ value less than zero implies a favorable Möbius transition state (i.e. reaction is π-exothermic). As an example, Hückel-calculated $^{o}p_{1,4}$ for butadiene **11** is -0.4472 which leads to the conclusion that disrotatory 1,4 closure (Hückel transition state) is disfavored and that conrotatory closure (Möbius transition state) is favored.

For neutral polyenes, their dications and dianions, those earlier conclusions for thermal reactions through Hückel transition states are all reversed for thermal closures through Möbius transition states.

$^{0}p_{i,k}$ Values and Photolyses

In organic photochemical reactions, one presumes, for present purposes, that photoexcitation will promote one electron from the HOMO to the LUMO. Hence, Hückel-level calculated π-bond orders for the photoexcited state will have unaltered contributions for all electron pairs lying below the HOMO. The nodal properties of a polyene HOMO can be easily anticipated, as pointed out earlier[16] and illustrated in Figure 5. The nodal properties of the corresponding polyene LUMO can be anticipated by bringing together a set of ethylene LUMOs so that each contact point introduces a bonding interaction.[16] Figure 14 presents the frontier molecular orbitals for octatetraene **5**.

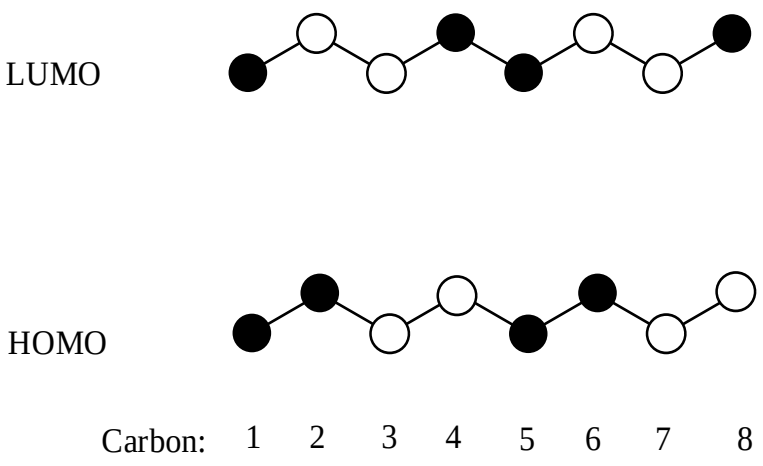

Fig. 14.

For non-alternant, cyclic transition states, $^{o}p_{i,k}$ equals $^{*}p_{i,k}$ and photoexcitation is expected to have no effect on the facility of ring formation i.e. it is not favored. In contrast, incipient alternant ring formation is profoundly affected by photoexcitation. When a given pair of polyene

centers, e.g. C_1 and C_6 in Figure 14, have an incipient bonding interaction in the HOMO they have an incipient antibonding interaction in the LUMO and *visa versa*. The absolute values of corresponding HOMO and LUMO coefficients are equal. Hence, the effect of the bonding electrons in the HOMO of the ground state is completely removed in the excited state. When the incipient bonding interaction in the HOMO is unfavorable, as it is for C_1C_4 in the HOMO of octatetraene **5** in Figure 14, photoexcitation facilitates concerted cyclization i.e. ${}^{*}p_{i,k} > {}^{o}p_{i,k}$. This is the case for all Hückel transition states that lead to 4J annulenes which bear even substituents. When the incipient bonding interaction in the HOMO is favorable, as it is for C_1C_6 in the HOMO of octatetraene **5** in Figure 14, photoexcitation impairs cyclization i.e. ${}^{*}p_{i,k} < {}^{o}p_{i,k}$.

When a given electrocyclic reaction produces an incipient alternant ring that bears a pair of odd substituents and when the reaction is weakly favored i.e. ${}^{o}p_{i,k} > 0$, as is the case for C_2C_7 in octatetraene **5**, photoexcitation further favors reaction i.e. $*p_{i,k} >> 0$. Hence, octatetraene **5** could close via disrotatory motion to introduce a new C_2C_7 bond along with cis stereochemistry in a weakly favored thermal process or the same closure to give the same stereochemistry could be carried out by means of a more strongly favored photochemical process.

Conventional frontier orbital arguments also find this cyclization to be allowed both thermally and photochemically but provide no basis for expecting the photochemical reaction to be superior (see Fig. 15).

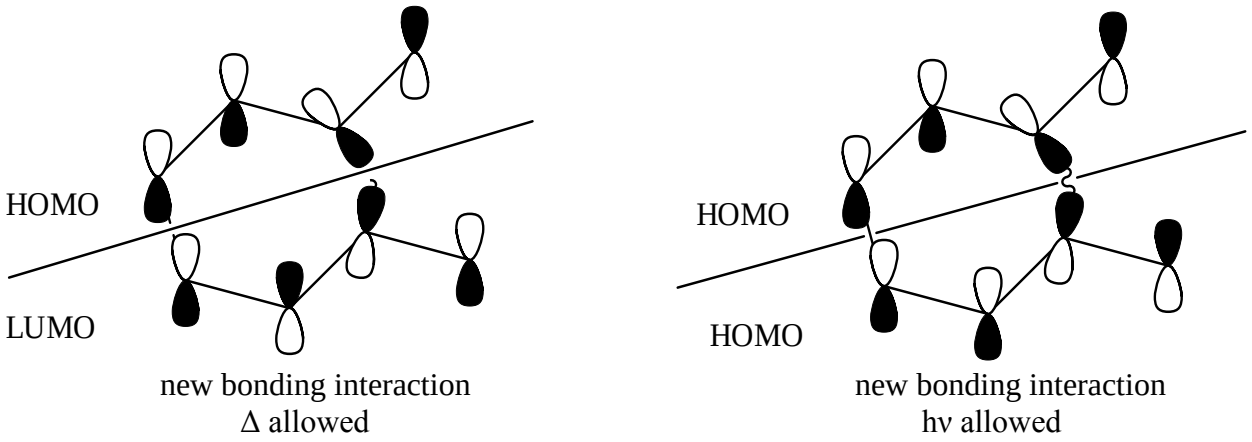

Fig. 15. Frontier orbital analysis leading to the conclusion that disrotatory closure to begin formation of a C_2C_7 bond is allowed both thermally and photochemically.

The disrotatory reaction envisioned in the preceding discussion is shown in Scheme 3.

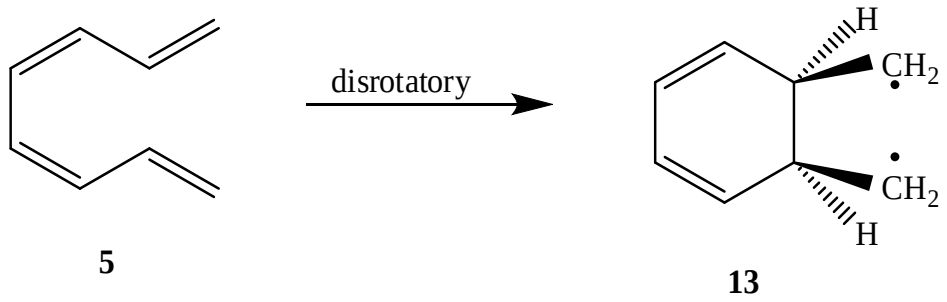

5 **13**

Scheme 3.

Figure 16A/B presents a correlation diagram that examines both thermal and photochemical disrotatory cyclization to produce the cyclohexadiene diradical **13** from octatetraene **5** (see Scheme 3).

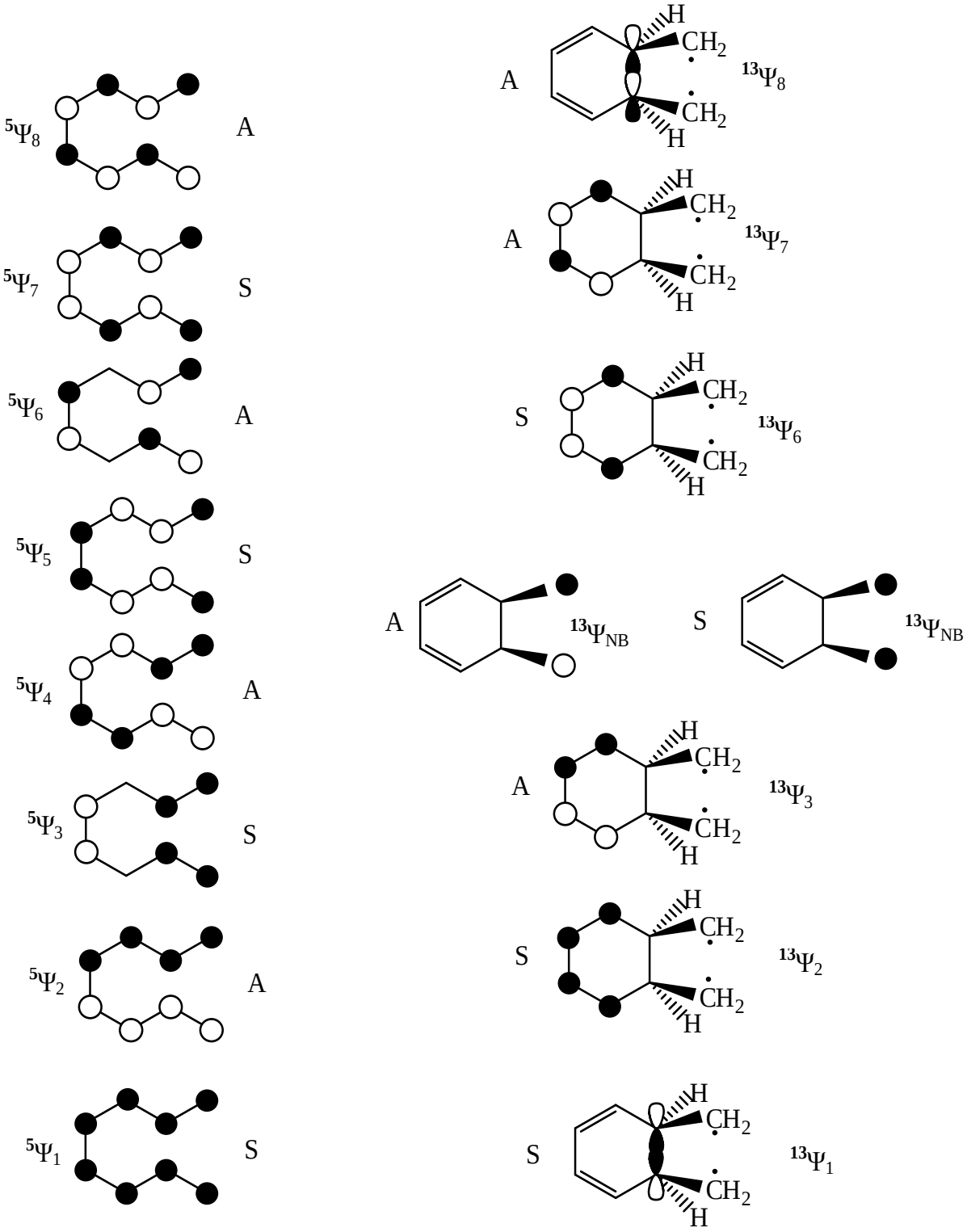

Fig. 16A. Mirror plane symmetries of the molecular orbitals of **5** and **13** for the double correlation diagram shown in Figure 16B. The plane in question is perpendicular to the molecular plane (e.g. octatetraene) and bisects the molecule into two C_4 segments.

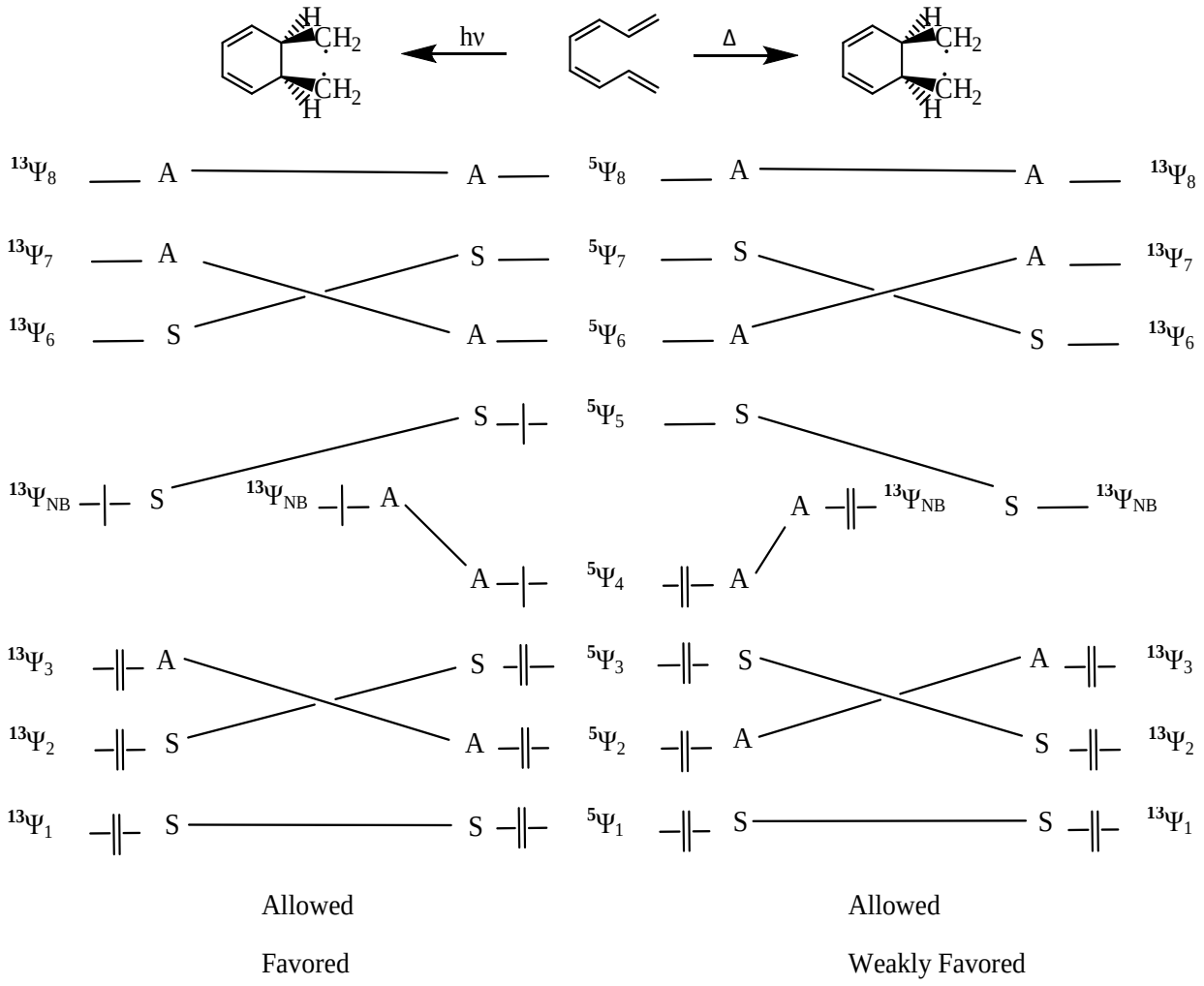

Fig. 16B. A correlation diagram showing that disrotatory electrocyclic conversion of **5 → 13** is weakly favored thermally and favored photochemically.

Typically, a correlation diagram for a forbidden process leads to the conclusion that a lower-energy orbital must remain vacant while a higher-energy orbital is occupied. Since the correlation diagram in Figure 16 does not lead to such a conclusion, the thermolysis (right-hand

side of Fig. 16B) is allowed. On the other hand, the product, **13**, has a degenerate pair of non-bonding molecular orbitals (NBMOs) so that double occupation of one, leaving the other vacant, violates Hund's Rule. Hence, the correlation diagram is consistent with the conclusions reached from $^{o}p_{i,k}$ and $^{*}p_{i,k}$ values, as noted in Figure 16B. Reactions through quinoid transition states provide a class of potentially concerted reactions which, in principle, are allowed thermally but should proceed photochemically to give the same product, including relative stereochemistry, with greater facility.

The Effect of More Than Two Odd Substituents on $^{o}p_{i,k}$ and $^{*}p_{i,k}$ Values

Thermal Reactions

An assessment of incipient ring formation for rings bearing even numbers of odd substituents, greater than two, cannot be done using electrocyclic closures of unbranched, acyclic polyene precursors. Hence, the FEM is not helpful here. Figure 17 provides Hückel-calculated $^{o}p_{i,k}$ values for pairs of polyenes showing that the incipient π-bond orders decrease sharply as the number of odd substituents, on the incipient alternant ring, increases. For this reason, incipient rings bearing more than two odd substituents will not be considered beyond the completion of this major section.

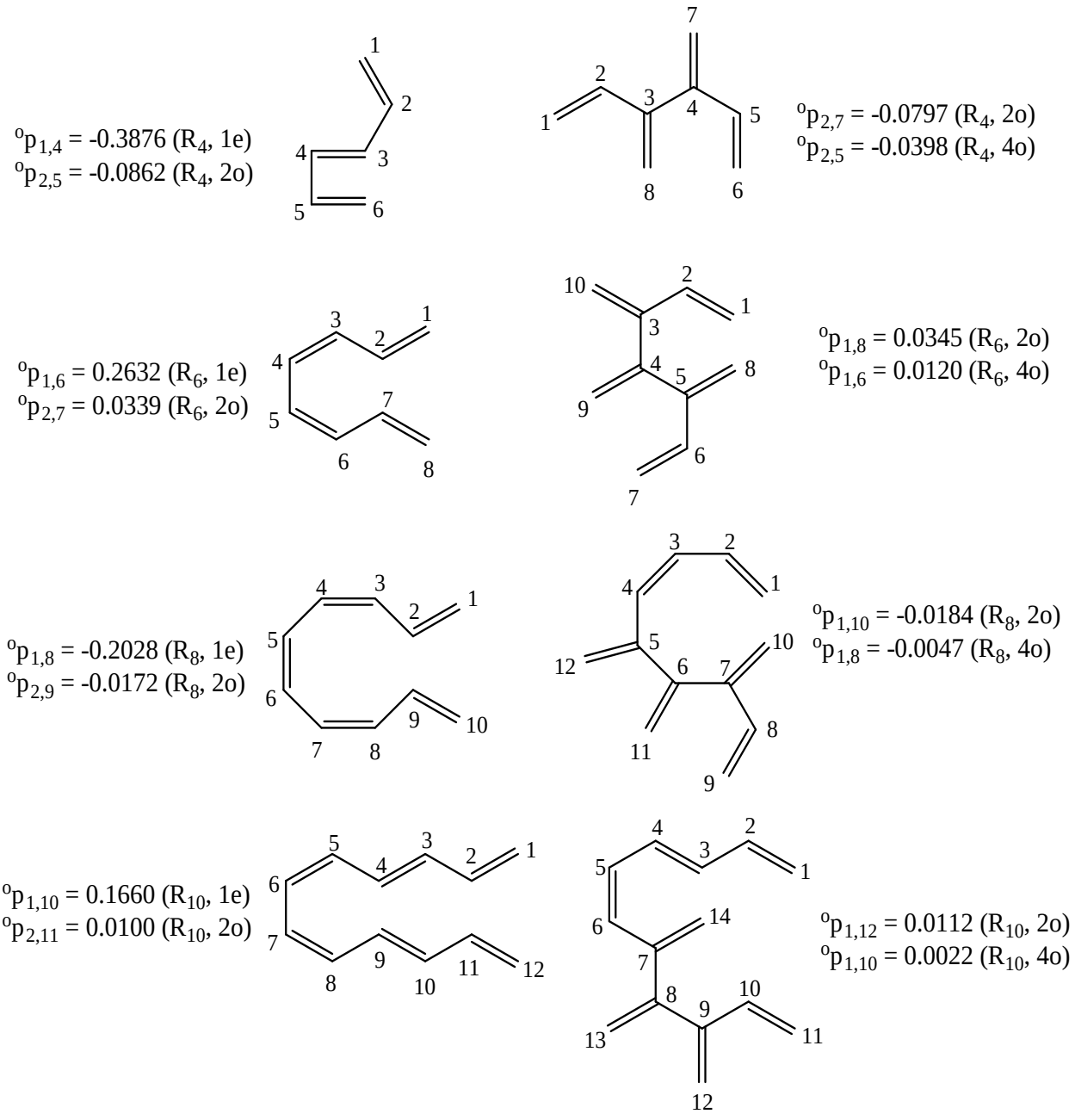

Fig. 17. Hückel-calculated $^{o}p_{i,k}$ values showing that more than two odd substituents on alternant circuits so diminishes their magnitude that the corresponding transition states are unlikely to be of interest. Note, terms in brackets designate incipient ring type e.g. (R_4, 2o) indicates an incipient 4-membered ring bearing two odd substituents.

Photochemical Reactions

In accord with the preceding discussion of photochemistry, closures that are impaired thermally by an incipient antibonding interaction in the HOMO are facilitated photochemically. Closures that are facilitated thermally by an incipient bonding interaction in the HOMO are impaired photochemically.

Figure 18 gives the structure for the C_{12} permethylene polyene **14** and Figure 19 shows three possible incipient C_6 closures available to it that bear increasing numbers of odd substituents.

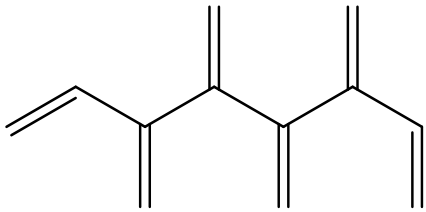

14

Fig. 18.

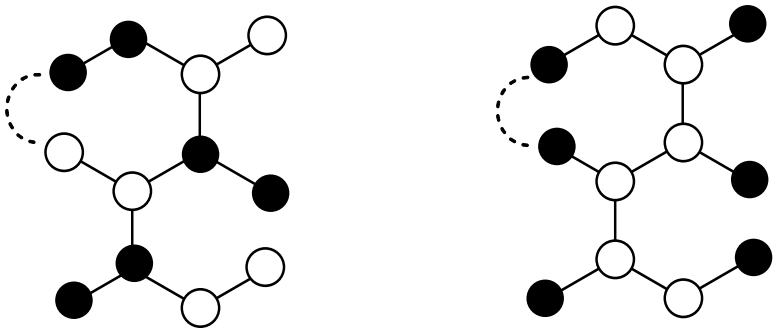

HOMO LUMO

$^{*}p_{i,k} > {}^{o}p_{i,k}$, photochemical closure superior

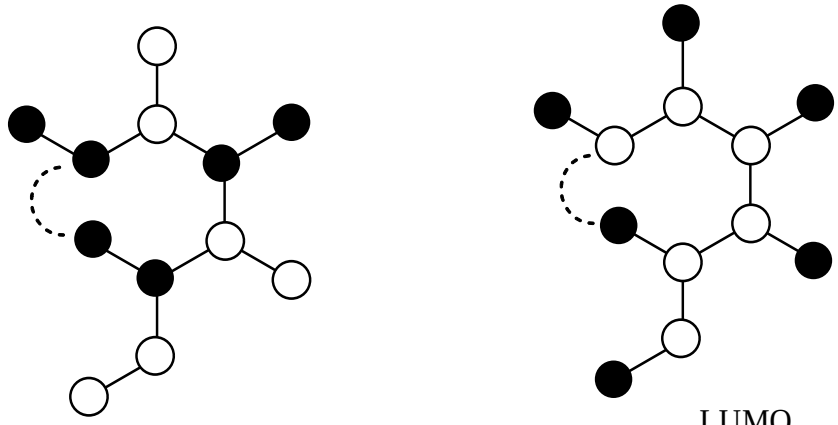

HOMO LUMO

$^{o}p_{i,k} > {}^{*}p_{i,k}$, thermal closure superior

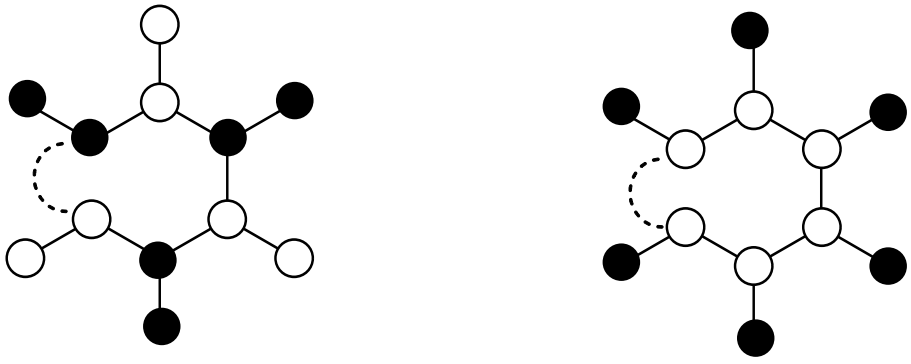

HOMO LUMO

$^{*}p_{i,k} > {}^{o}p_{i,k}$, photochemical closure superior

Fig. 19. Qualitative FMO deduction that increasing pairs of odd substituents cause preference for closure to alternate between thermal and photochemical pathways.

As for Figure 17, Figure 19 results involve incipient π-bond orders that are very modest.

General Selection Rules

The foregoing discussion presents a new basis, ${}^{o}p_{i,k}$ and ${}^{*}p_{i,k}$ values, for the assessment of concerted reaction transition states. This basis has been applied to exemplary electrocyclic reactions but is applicable to all those pericyclic reactions encompassed by the established Hückel/Möbius analyses. As an example, the electrocyclic closure of hexatriene **1** (Hückel transition state) and the cycloaddition of ethylene to butadiene **11** (Hückel transition state) may both be viewed as proceeding through favored [4N+2(es)] transition states.

Table 1 presents a convenient summary of the conclusions we have reached about monocyclic transition states.

Table 1. General selection rules for monocyclic transition states of concerted reactions

Incipient Ring Type[B] (odd/ even substituents)	Hückel Transition States[A] Δ[C]	Hückel Transition States[A] hν[C]	Möbius Transition States[A] Δ[C]	Möbius Transition States[A] hν[C]
4J+2(es)	F	D	D	F
4J+2(2os)	WF	F	WD	D
$4J+2(es)^{2+/2-}$	D	-	F	-
$4J+2(2os)^{2+/2-}$	F	-	D	-
4J+3/5(es)	-	-	-	-
$4J+3(es)^{+}/4J+5(es)^{-}$	F	-	D	-
$4J+3(es)^{-}/4J+5(es)^{+}$	D	-	F	-
$4J+3(os)^{+/-}/4J+5(os)^{+/-}$	-	-	-	-
$4J(es)^{2+/2-}$	F	-	D	-
$4J(2os)^{2+/2-}$	D	-	F	-
4J(2os)	WD	D	WF	F
4J(es)	D	F	F	D

[A] F = Favored, D= Disfavored, WF= Weakly Favored, WD= Weakly Disfavored

[B] An example of incipient ring type: 4J+2(es) means a transition state which features a monocyclic p-orbital array containing 4J+2 π electrons in an incipient ring that bears only even substituents (includes unsubstituted rings).

[C] Δ = thermal reaction, hν = photochemical reaction

The conclusions reached in Table 1 entirely subsume all of the usual Hückel/Möbius conclusions and add new conclusions for quinoid monocyclic transition states. In contrast to the established approach, the present approach permits direct assessments of photochemical transition states. The present method obviates the need to base conclusions entirely on frontier orbitals and their electrons and eliminates the need to examine concerted unimolecular reactions by arbitrarily dividing a polyene π system into a HOMO portion and a LUMO portion.

Size Effects

Hückel-level Parameters

Established Hückel/Möbius transition-state assessments rely on analogies with ground-state annulenes. In reality, as annulenes grow in size, their π systems become more and more like those of acyclic, unbranched polyenes. Traditional Hückel calculations characterize hydrocarbon π systems by means of Classical Resonance Energies which compare E_π for the molecule of interest with the total E_π for the appropriate number of ethylene molecules e.g. the Classical Resonance Energy for hexatriene **1** is -0.9878β (E_π(3 ethylenes): 6α +6β less E_π(hexatriene): 6α +6.9878β).

Classical Resonance Energies invite direct comparison of molecules which have different numbers of carbon atoms because they appear to be independent of size. They remain particularly troublesome for 4J annulenes all of which are Hückel triplets. When $J \geq 2$, 4J annulenes have favorable Classical Resonance Energies, implying that the annulenes have superior stabilization and that the corresponding 4J transition states should be favorable. Dewar shifted the reference structures for cyclic hydrocarbons to acyclic polyenes which provides some improvement e.g. the Dewar Resonance Energy for benzene is 1β (E_π(benzene): 6α +8β less E_π(hexatriene): 6α +7β). Nonetheless, Dewar Resonance Energies are also favorable for larger 4J annulenes e.g. cyclododecahexaene **15** has a DRE of 0.3360β.

Related Topological Resonance Energies give negative TRE values for all 4J annulenes but one still has to divide TRE values by the number of π electrons [gives TRE(PE)] in order to fully counter the Hückel-level tendency to favor larger π systems.[19] The use of TRE(PE) values permits direct comparisons of differently-sized π systems. Unfortunately, TRE(PE) numbers are unreasonable for some structure types.[20]

The current approach to transition state assessment does not rely on analogy with annulenoid π systems. Incipient 4J circuits are always associated with ${}^{o}p_{i,k} < 0$ and incipient 4J+2 circuits are always associated with ${}^{o}p_{i,k} > 0$. No corrective steps need be taken. As incipient rings grow in size, $|{}^{o}p_{i,k}|$ values shrink, indicating that the transition states are less and less advantaged/disadvantaged. One can anticipate that result in the following way.

For any unbranched, acyclic polyene, the absolute value of any FEM coefficient falls between the sine values of 0˚ and 90˚. From the curvature of a sine function between these angles, one can see that the differences between large coefficient pairs is small compared to the difference between small coefficient pairs. As an example, α,ω closure for decapentaene **6** has a transition state assessment dependent upon ${}^{o}p_{1,10}$ [see Eqn (15)].

$$ {}^{o}p_{1,10} = 2a^2 - 2b^2 + 2c^2 - 2d^2 + 2e^2 \qquad (15) $$

The differences between the last pair of terms and the penultimate pair is substantial [see Eqns (16), (17)].

$$ |-2d^2 + 2e^2| = 0.0803 \qquad (16) $$
$$ |-2b^2 + 2c^2| = 0.4741 \qquad (17) $$

One can now say that ${}^{o}p_{1,10}$ has three major terms rather like the ${}^{o}p_{1,6}$ expression for α,ω closure of hexatriene **1**. Each of the three terms for these two incipient π-bond orders have the same numerator (bm180˚) but different denominators (2n+1 is only 7 for hexatriene **1** but it is 11 for decapentaene **6**). Thus ${}^{o}p_{1,10}$ for **6** is smaller than ${}^{o}p_{1,6}$ for **1**. A parallel argument may be made comparing α,ω closures of the C_{10} and C_{14} unbranched polyenes and so on. Note that ${}^{o}p_{i,k}$ values employing normalized coefficients, in place of FEM coefficients, will offer further disadvantage to large incipient rings because the normalization coefficients shrink with increasing polyene size (see Methods).

Experimental Results

It is often the case that concerted reactions lead to the preferred formation of smaller rings, particularly R_6, in preference to larger rings e.g. R_{10}. Scheme 4 offers an established example.[21]

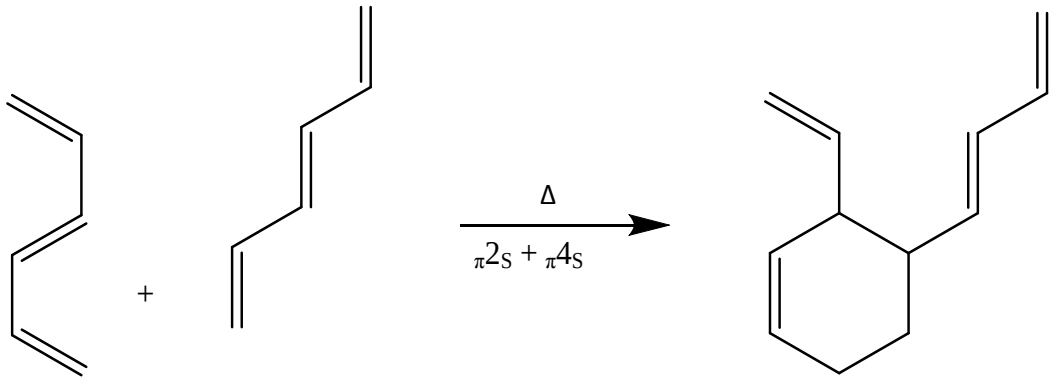

Scheme 4.

There is, however, a fascinating subset of cycloaddition reactions involving conformationally constrained (i.e. cyclic) reaction components. An example is given in Scheme 5.[22,23]

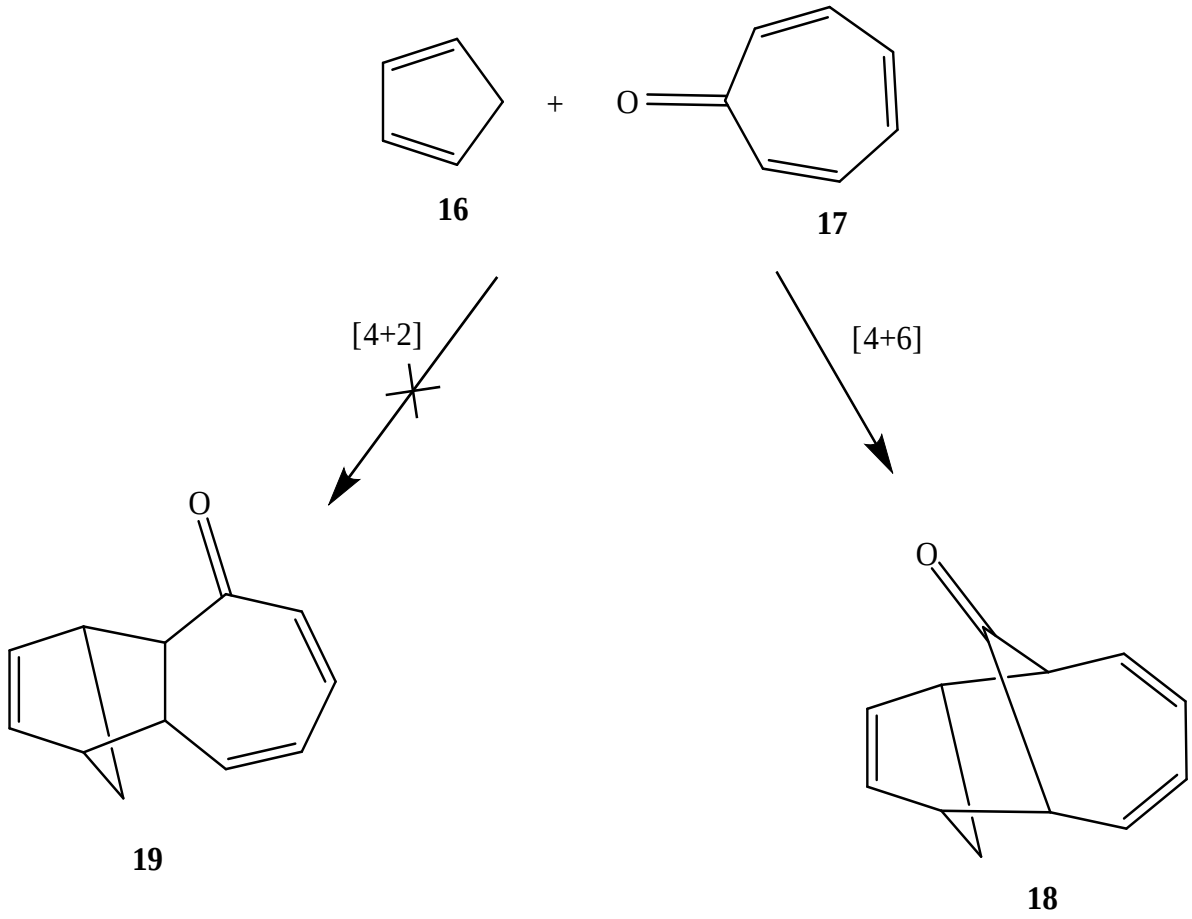

Scheme 5. Experimental outcome of the cycloaddition reaction of cyclopentadiene **16** with tropinone **17**.

Not uncommonly, these constrained reactants produce the product whose allowed transition state features the largest continuous p-orbital array. Fleming[24] has offered a detailed rationale for the outcome of the reaction in Scheme 5 using semiempirical frontier orbital coefficients available at that time (1976).

When $^{o}p_{i,k}$ values were determined for a pair of model electrocyclic reactions, both Hückel and PM3 values indicated that the transition state with the smaller p-orbital array should be preferred

(see Fig. 20).

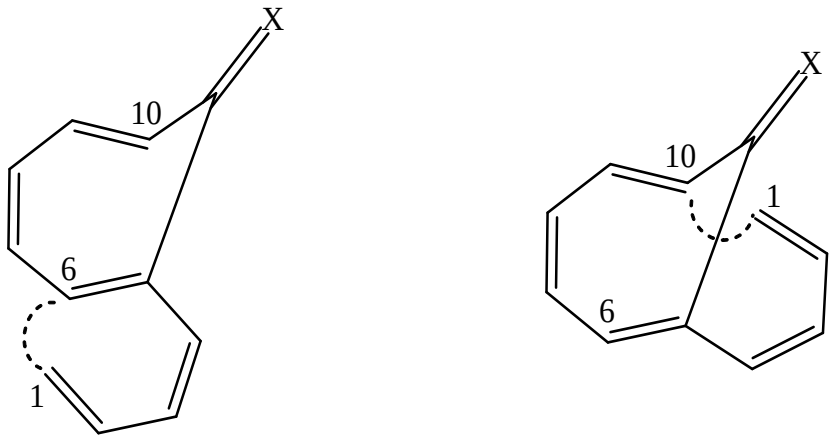

20 X = CH_2; Hückel $^{o}p_{1,6} = 0.2194$ $^{o}p_{1,10} = 0.1587$

21 X = O; PM3 $^{o}p_{1,6} = 0.0968$ $^{o}p_{1,10} = 0.0285$

Fig. 20. Hückel and PM3 $^{o}p_{i,k}$ values showing that the π systems in **20** and **21** both favor electrocyclic closure through an incipient cyclic, R_6 transition state.

Furthermore, when Hückel-level cycloaddition-transition-state modeling was undertaken (all bond integrals set at 1β except those for the partially-formed bonds which were set at 0.1β), the incipient, cyclic (R_6) transition state is again found to be preferred (see Fig. 21).

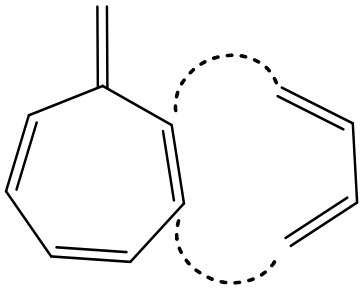

$E_\pi = 12\alpha + 14.4826\beta$

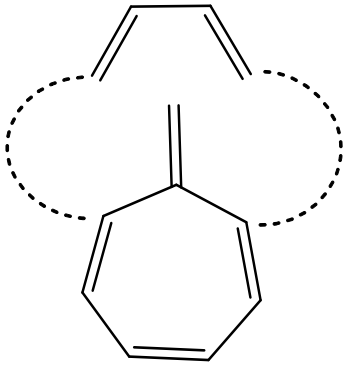

$E_\pi = 12\alpha + 14.4816\beta$

Fig. 21. Hückel-level transition-state modeling which shows that the 4+2 addition is preferred over the 4+6 addition

Moreover, modern semiempirical frontier molecular orbital coefficients do not support either the experimental outcome shown in Scheme 5 or the 1976 frontier orbital-based analysis. For tropinone **17** and butadiene **11**, the smaller HOMO-LUMO energy difference is associated with the tropinone LUMO and the butadiene HOMO. Appropriate PM3 coefficients are available in Figure 22.

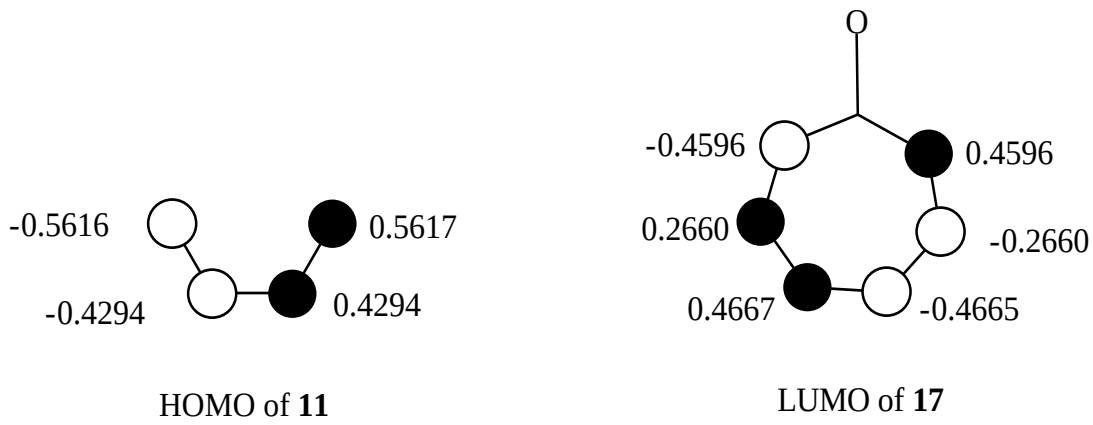

Fig. 22. PM3 frontier orbital coefficients for tropinone **17** and butadiene **11.**

From Fleming's discussion,[24] one may assess competing cycloadditions by multiplying together coefficient pairs at the reacting centers and squaring their sum.[9-11] The appropriate calculations, using PM3 coefficients are shown in Eqns (18) and (19).

$$[4+6] \text{ cycloaddition } \Sigma a^2 = [\ 2(0.4596 \times 0.5616)]^2 = 0.2664 \quad (18)$$

$$[4+2] \text{ cycloaddition } \Sigma a^2 = [\ 2(0.4667 \times 0.5616)]^2 = 0.2747 \quad (19)$$

Hence, the preferred outcome for a very close relative of the Scheme 5 reaction, based on modern semiempirical coefficients for the appropriate frontier orbitals (given in Fig. 22) is shown in Scheme 6.

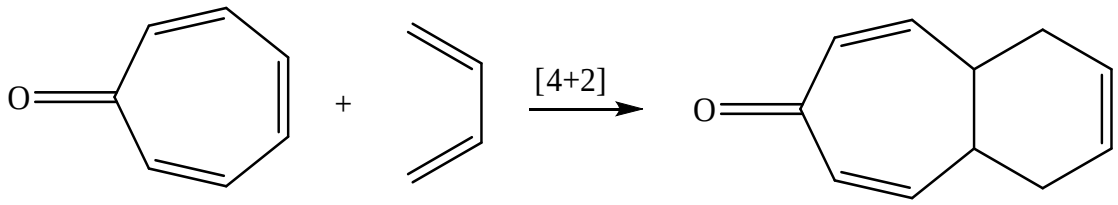

17 **11**

Scheme 6. The frontier-orbital-based (PM3 coefficients) expectation for a close relative of the Scheme 5 reaction.

On the basis of the foregoing discussion, the outcome of reactions, like those in Scheme 5 which feature competing, allowed pathways, seem likely to be subject to control by factors such as enthalpies of formation, steric crowding and ring strain.

There are known counterexamples in which conformationally-constrained reactants form products, through the smaller π system, preferentially. Interestingly, the example in Scheme 7 which favors the 4+2 pathway thermally, pursues the 8+2 pathway photochemically.[25]

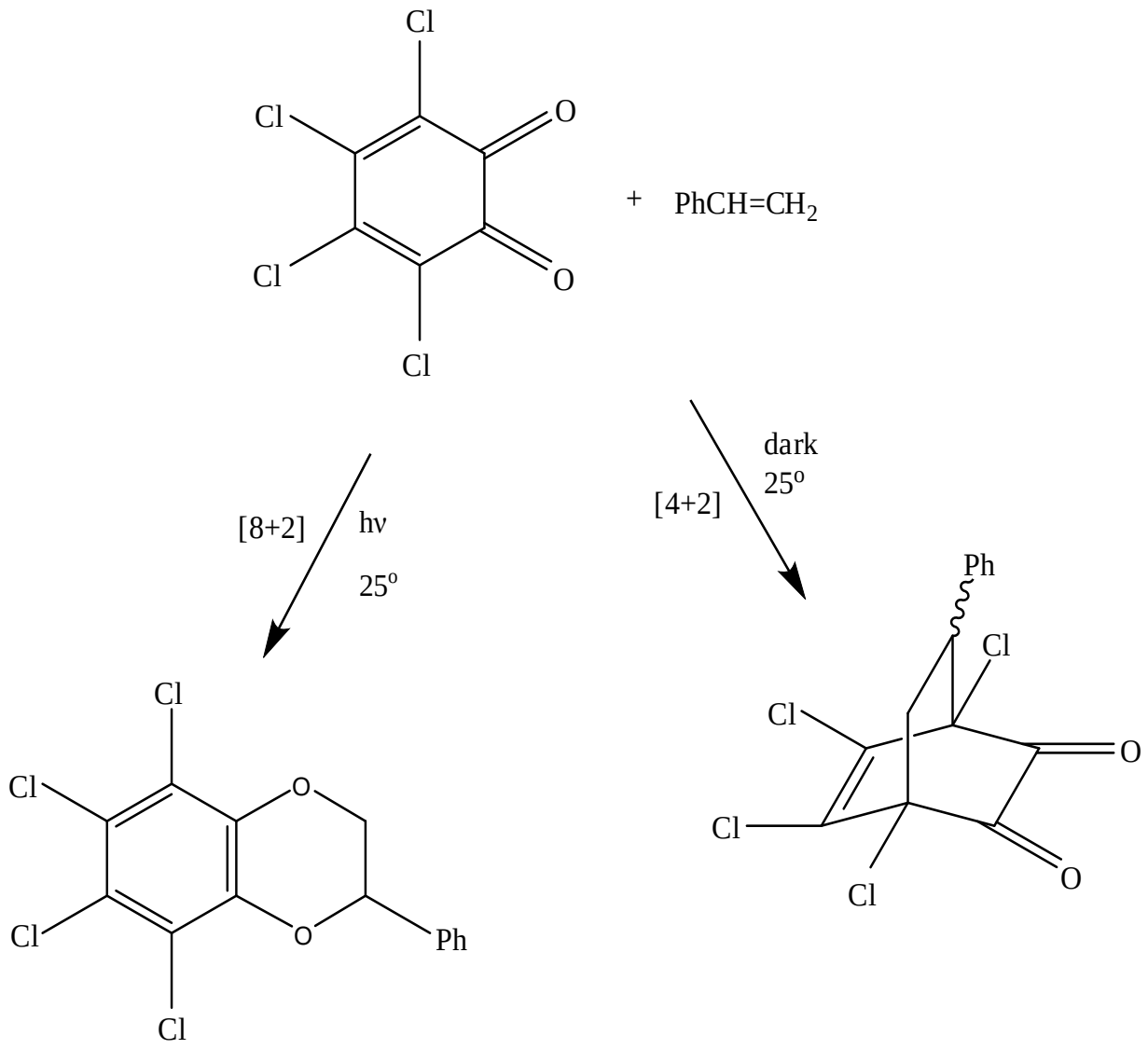

Scheme 7.

Note that the [4+2] pathway (Scheme 7) is favored thermally even though the [8+2] pathway aromatizes the tetrachloro ring. Anticipating which of several competing, allowed pathways will be observed cannot be done consistently without allowing for reaction features that lie outside the domain of the π system alone.

Selected Problematic Reactions

As outlined in the Introduction and illustrated in Scheme 2, cyclooctatetraene **3** is in equilibrium with the cis-fused bicyclooctatriene **4**. Disrotatory closure/opening is observed thermally. A conventional Hückel/Möbius transition-state assessment leads to an ambiguous conclusion, if the structure of **3** is assumed to be planar. Furthermore, $^{o}p_{1,4}$ (see Scheme 2) for planar cyclooctatetraene **3** is -0.1036 indicating that disrotatory closure is weakly disfavored.

Traditional Zeroth Order Hückel calculations find that planar, regular-octagonal cyclooctatetraene **3** is a ground-state triplet and experimentally it is known to be a non-planar, ground-state singlet. Following a Least Motion argument,[26] a suitable conformation for cyclooctatetraene **3** to reach the transition state for the formation of **4** is pictured in Figure 23.

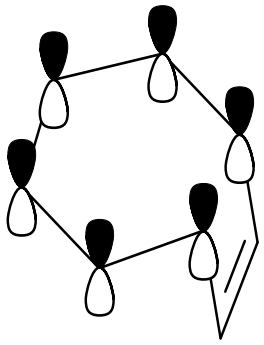

Fig. 23. A suitable conformation for disrotatory electrocyclic conversion of **3** → **4** (see Scheme 2).

The folded conformation envisioned in Figure 23 is associated with a discontinuity in the p-orbital overlap in the incipient R_4 transition state entertained earlier in Figure 2. On the other hand, transition-state analysis in terms of an R_6 p-orbital array is now reasonable on conformational grounds.

In sharp contrast to cyclooctatetraene **3**, planar benzocyclooctatetraene **22** is both a Hückel and a PM3 singlet. Scheme 8 shows three possible topologies for thermal electrocyclic reaction in the cyclooctatetraene ring.

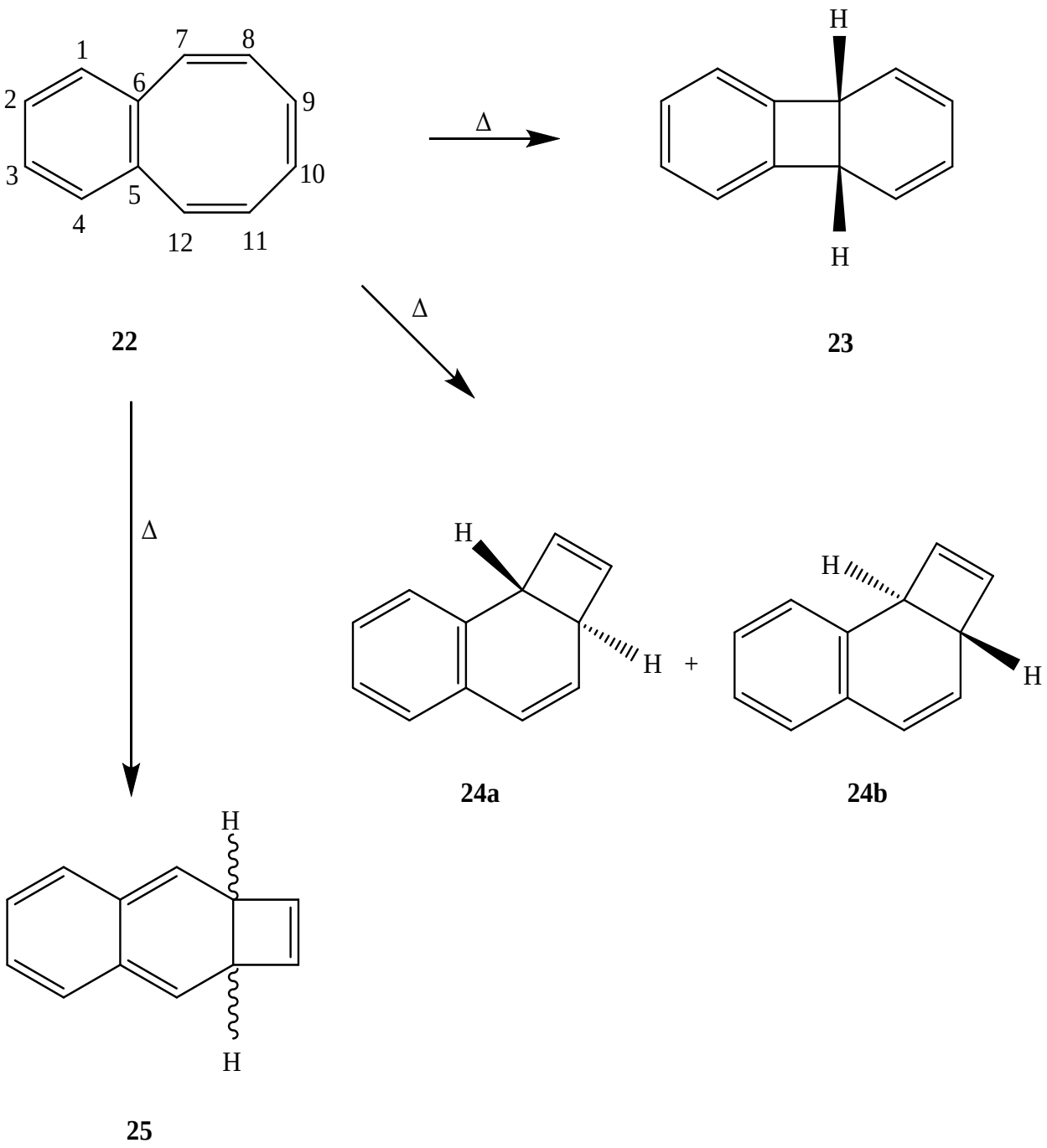

Scheme 8. Potentially competing electrocyclic closures in R_8 of benzocyclooctatetraene **22** and the stereochemistries expected on the basis of ${}^{o}p_{i,k}$ values.

Because it would be unwise to treat the p-orbitals of the transition state for the formation of any of the products in Scheme 8 as a monocyclic array, application of the present approach to assess those thermal electrocyclic closures requires appropriate $^{o}p_{i,k}$ values. At the Hückel level, they are: $^{o}p_{7,12} = 0.1897$; $^{o}p_{7,10} = -0.3468$; $^{o}p_{8,11} = 0.0109$. Hence, disrotatory closure is favored in the process leading to **23** but disfavored for the reaction that gives **24a**, **24b**. On the other hand, conrotatory closure is disfavored for the formation of **23** and favored for the formation of **24a**, **24b**. The formation of **25** should not be competitive for either conrotatory or disrotatory pathways.

An interesting pair of thermolyses have been reported[27] (see Scheme 9).

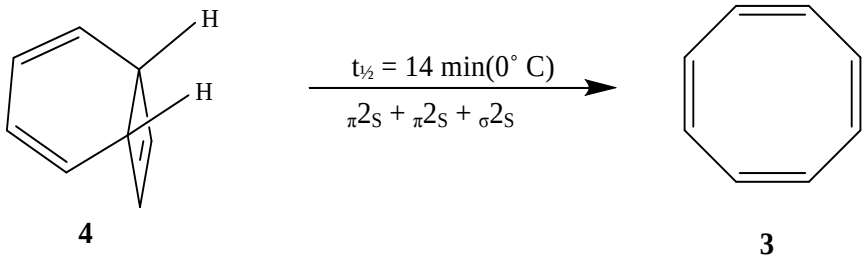

4 **3**

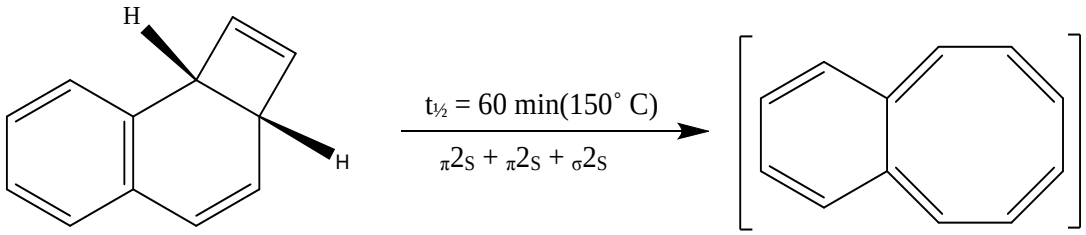

24c

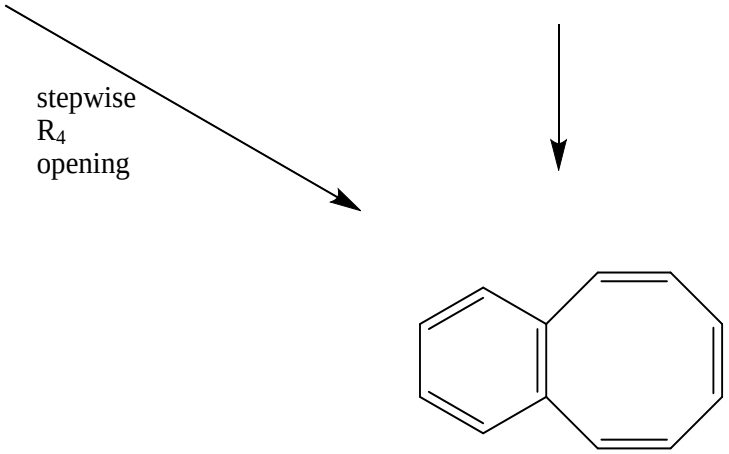

22

Scheme 9. Experimental results from reference 27.

The stark difference in conditions for these apparently closely-related thermolyses (Scheme 9) presents a challenge to rationalize. Bender[27] offers the suggestion that the thermal conversion of **24c** into **22** must proceed through a non-aromatic intermediate (shown in brackets in Scheme 9), thus making it more difficult. Nonetheless, reaction conditions are sufficiently different that he also proposed that the higher temperature pyrolysis may proceed in a stepwise fashion, presumably through a diradical, to give benzocyclooctatetraene **22**.

Given (i) the Principle of Microscopic Reversibility[28] and (ii) our ${}^{o}p_{7,10}$ value (Scheme 8), the first step of the second reaction is thermally disfavored (forbidden) and should require rugged conditions. Consistent with that view, ${}^{*}p_{7,10}$ is increased by 0.2714 realtive to ${}^{o}p_{7,10}$, so that photochemical opening is expected to be significantly facilitated.

Experimentally,[27] direct photolysis of the starting tricycle **24c** in Scheme 9 did, indeed, give some benzocyclooctatetraene **22**. It may have formed, in part, by disrotatory opening but labelling experiments implicated diradical intermediates, hence, a concerted hypothesis is not necessary to rationalize part of the observed results.

The isomerization of the proposed intermediate's R_8 would be thermally forbidden (traditional Hückel/Möbius analysis). Now, ${}^{o}p_{i,k}$ and ${}^{*}p_{i,k}$ values offer a straightforward rationale for the Scheme 9 results and give unambiguous support to the notion that the pyrolysis of **24c** may produce **22** through a diradical precursor. In Woodward-Hoffmann terms,[1] the first step in the second reaction of Scheme 9 might better be classified as a ${}_{\pi}2_S + {}_{\sigma}2_S$ process, although implicitly neglecting any portion of the π system (i.e. treating a polycyclic p-orbital array as though it were a monocyclic array) may easily deprive one of key insights.

A Comparison of Hückel-calculated and PM3 $^{o}p_{i,k}$ Values

Hückel-calculated $^{o}p_{i,k}$ values for acyclic, unbranched polyenes and polyenyls have been used throughout this report. To explore possible differences between those $^{o}p_{i,k}$ values obtained from traditional Hückel calculations and those obtained from modern PM3 semiempirical calculations, we have obtained both types for the C_{18} unbranched, acyclic polyene. The results are presented in Table 2.

Table 2. Hückel and PM3 $^{o}p_{i,k}$ values for the unbranched, acyclic polyene (C_{18})

Incipient Ring^{A,B,C,D} (Substituents)	i,k	Hückel $^{o}p_{i,k}$	PM3 $^{o}p_{i,k}$
R_4(es)	1,4	-0.3453	-0.2598
R_4(es)	3,6	-0.2921	-0.2570
R_4(es)	5,8	-0.2741	-0.2565
R_4(es)	7,10	-0.2677	-0.2563
R_4(2os)	2,5	-0.1181	-0.0306
R_4(2os)	4,7	-0.1476	-0.0349
R_4(2os)	6,9	-0.1587	-0.0357
R_4(2os)	8,11	-0.1617	-0.0361
R_6(es)	1,6	0.2271	0.1022
R_6(es)	3,8	0.1977	0.1027
R_6(es)	5,10	0.1866	0.1028
R_6(es)	7,12	0.1836	0.1028
R_6(2os)	2,7	0.0533	0.0075
R_6(2os)	4,9	0.0711	0.0082
R_6(2os)	6,11	0.0776	0.0092
R_8(es)	1,8	-0.1739	-0.0448
R_8(es)	3,10	-0.1561	-0.0452
R_8(es)	5,12	-0.1495	-0.0455
R_8(2os)	2,9	-0.0295	-0.0023
R_8(2os)	4,11	-0.0405	-0.0028
R_8(2os)	6,13	-0.0435	-0.0029
R_{10}(es)	1,10	0.1444	0.0206
R_{10}(es)	3,12	0.1333	0.0209

R_{10}(es)	5,14	0.1304	0.0210
R_{10}(2os)	2,11	0.0178	0.0008
R_{10}(2os)	4,13	0.0243	0.0008
R_{12}(es)	1,12	-0.1265	-0.0097
R_{12}(es)	3,14	-0.1200	-0.0099
R_{12}(2os)	2,13	-0.0111	-0.0003
R_{12}(2os)	4,15	-0.0141	-0.0003
R_{14}(es)	1,14	0.1155	0.0047
R_{14}(es)	3,16	0.1124	0.0047
R_{14}(2os)	2,15	0.0065	0.0002
R_{16}(es)	1,16	-0.1089	-0.0017
R_{16}(2os)	2,17	-0.0030	-0.0000
R_{18}(es)	1,18	0.1059	0.0010

[A] R_4 represents a four-membered ring, R_6 a six-membered ring and so on.
[B] (es) means that the ring bears only even, unbranched, acyclic substituents.
[C] (2os) means that the ring bears two odd, unbranched, acyclic substituents.
[D] Each incipient non-alternant monocycle, had one odd substituent and a $^{o}p_{i,k}$ value = 0 at both Hückel and PM3 levels of theory.

Generally, $^{o}p_{i,k}$ values from PM3 computations are smaller than the corresponding Hückel values. As ring size increases, PM3 $^{o}p_{i,k}$ values reach zero sooner e.g. both PM3 $^{o}p_{i,k}$ values for R_{16}(2os) and R_{18}(es) are zero while the Hückel numbers suggest that electrocyclic reactions may produce 18-membered rings. Although their formation is still favored, PM3 calculations imply that electrocyclic reactions would have difficulty forming R_{14}(es) systems.

Notwithstanding the pronounced bias in PM3 values which favors smaller rings, PM3 and Hückel numbers support the same conclusions about which transition states are favored (F), disfavored (D), weakly favored (WF) or weakly disfavored (D).

Formal Analytical Procedure for Transition-state Evaluation Based on ${}^{o}p_{i,k}$ Values

In several places, the current report presents traditional Hückel/Möbius evaluations for transition states which feature a monocyclic array of p-orbitals (e.g. see Figs. 1 and 2). From Table 1, it is now clear that prudent assessments of such transition states should take note of the presence/absence of a pair of odd substituents prior to reaching a conclusion. That done, Table 1 provides appropriate conclusions.

When a transition state features a polycyclic p-orbital array, particularly for fused polycyclic systems, an attempt to assess it in terms of a monocyclic array may be both convenient and unwise. In such a case, the key ${}^{o}p_{i,k}$ values may be simply obtained from traditional Hückel calculations.

Figure 24 gives exemplary transition states, one monocyclic and one polycyclic p-orbital array along with appropriate evaluations using the current method. For a polycyclic array, it is good practice to confirm a conclusion, based on a ${}^{o}p_{i,k}$ value, by comparing it with the corresponding ${}^{*}p_{i,k}$ value and *visa versa*.

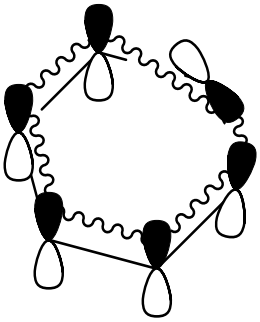

0 nodes, Hückel array
monocyclic, 4J+2(es)

Δ F

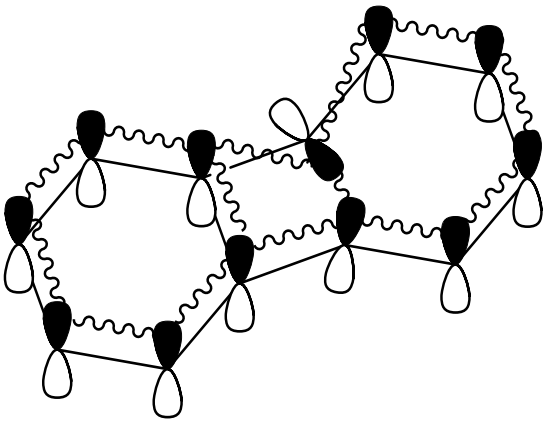

0 nodes, Hückel array
polycyclic, $^{0}p_{i,k} = 0.1897$, $^{*}p_{i,k} = -0.1151$

Δ F

Fig. 24. Exemplary transition-state assessments based upon $^{o}p_{i,k}$ and/or $^{*}p_{i,k}$ values. The wavy lines indicate orbital overlap.

Conclusions

A new approach to the assessment of Hückel/Möbius transition states has been described. It employs ${}^{o}p_{i,k}$ and ${}^{*}p_{i,k}$ values, associated with the starting structure, to classify transition states as F (favored), D (disfavored), WF (weakly favored) or WD (weakly disfavored). The approach, developed by explicitly considering electrocyclic reactions, provides conclusions that are readily applied to other classes of concerted reactions e.g. sigmatropic rearrangements. The development of this approach is reminiscent of the development of FMO arguments which, initially, explicitly examined cycloadditions and were then extended to many unimolecular reactions.

The present method obviates the need to represent all transition states as monocyclic p-orbital arrays. It offers routine capability for quinoid transition state assessments and has no dependence on Möbius annulenes. Arguments rely upon ${}^{o}p_{i,k}$ and ${}^{*}p_{i,k}$ values and do not depend upon Hückel eigenvalues which are known to be unreliable. An analytical method for the direct assessment of appropriate photochemical pathways has been devised. The current method is applicable to concerted reactions regardless of symmetry considerations. All π electrons and bonding orbitals play a role in reaching conclusions by means of ${}^{o}p_{i,k}$ and ${}^{*}p_{i,k}$ values.

Acknowledgements

We gratefully acknowledge technical assistance from B. McNally.

References

[1] R.B. Woodward, R. Hoffmann, *Angew. Chem. Int. Ed. Engl.* **1969**, *8*, 1.

[2] K. Fukui, *Acc. Chem. Res.* **1971**, *4*, 57.

[3] M.J.S. Dewar, *Angew. Chem. Int. Ed. Engl.* **1971,** *10*, 761.

[4] H.E. Zimmerman, *Acc. Chem. Res.* **1971**, *4*, 272.

[5] H.E. Zimmerman, *Tetrahedron*, **1982,** *38*, 753.

[6] R.F. Langler, *J. Chem. Ed.* **1996**, *73*, 899.

[7] A. Frost, B. Musulin, *J. Phys. Chem.* **1953**, *21*, 572.

[8] H.E. Zimmerman, *Pericyclic Reactions, Vol. 1* Ed. A. Marchand, R.E. Lehr, **1977**, pp 63,64 (Academic Press: New York, NY).

[9] G. Klopman, *J. Am. Chem. Soc.* **1968**, *90*, 223.

[10] L. Salem, *J. Am. Chem. Soc.* **1968**, *90*, 543.

[11] L. Salem, *J. Am. Chem. Soc.* **1968** *90*, 553.

[12] R.F. Langler, *Aust. J. Chem.* **2001**, *54*, 261.

[13] H.H. Jaffe, *J. Chem. Phys.* **1952**, *20*, 1646 and references therein.

[14] H.H. Jaffe, *J. Chem. Phys.* **1953**, *21*, 1287 and references therein.

[15] E. Heilbronner, *Tetrahedron Lett.* **1964**, 1923.

[16] J.C. Baum, E.D. Martin, J.L. Ginsburg, R.F. Langler, *Can. J. Chem.* **1995**, *73*, 1719.

[17] M.J.S. Dewar, R.C. Dougherty, *The PMO Theory of Organic Chemistry* **1975**, p 77 (Plenum: New York, NY).

[18] J.R. Dias, *Molecular Orbital Calculations Using Chemical Graph Theory* **1993** (Springer-Verlag: Heidelberg).

[19] N. Trinajstic, *Chemical Graph Theory, 2nd Ed.* **1992**, pp 125-156.

[20] R.F. Langler, *Aust. J. Chem.* **1991**, *44*, 297.

[21] M.S. Kharasch, E. Sternfeld, *J. Am. Chem. Soc.* **1939**, *61*, 2318.

[22] R.C. Cookson, B.V. Drake, J. Hudee, A. Morrison, *J. Chem. Soc.*, *Chem. Commun.* **1966**, 15.

[23] S. Ito, Y. Fujise, T. Okuda, Y. Inoue, *Bull. Chem. Soc. Jpn.* **1966**, *39*, 135.

[24] I. Fleming, *Frontier Orbitals and Organic Chemical Reactions* **1976**, p. 173 (Wiley: New York, NY).

[25] A. Schoenberg, N. Latif, *J. Chem. Soc.* **1952**, 446.

[26] J. Hine, *J. Org. Chem.* **1966**, *31*, 1236.

[27] C.O. Bender, *Can. J. Chem.* **1996**, *74*, 32.

[28] A.C. Cope, A.C. Haven, F.L. Ramo, E.R. Trumball, *J. Am. Chem. Soc.* **1952**, *74*, 4867.